Research Report R81-13

Order No. 699

PB82-147893

NSF/CEE-81060

AN EXPLICIT SOLUTION FOR THE GREEN FUNCTIONS FOR DYNAMIC LOADS IN LAYERED MEDIA

by

EDUARDO KAUSEL

DEPARTMENT
OF
CIVIL
ENGINEERING

SCHOOL OF ENGINEERING
MASSACHUSETTS INSTITUTE OF TECHNOLOGY
Cambridge, Massachusetts 02139

May 1981

Sponsored by the National Science Foundation
Division of Problem-Focused Research
Grant PFR 80-12336

Additional Copies May Be Obtained From:

National Technical Information Service
U. S. Department of Commerce
5285 Port Royal Road
Springfield, Virginia 22161

Massachusetts Institute of Technology
Department of Civil Engineering
Constructed Facilities Division
Cambridge, Massachusetts 02139

AN EXPLICIT SOLUTION FOR THE GREEN FUNCTIONS FOR DYNAMIC LOADS IN LAYERED MEDIA

by

Eduardo Kausel

May 1981

Sponsored by the National Science Foundation
Division of Problem-Focused Research
Grant PFR 80-12338

Publication No. R81-13 Order No. 699

Table of Contents

Acknowledgement

This is the first report issued under the research project entitled "Dynamic Behavior of Embedded Foundations," The project is supported by the National Science Foundation, Division of Problem-Focused Research Applications, under Grant PFR 80-12338.

Dr. William Hakala is the cognizant NSF program official, and his support is gratefully acknowledged.

The opinions, findings and conclusions or recommendations expressed in this report are those of the author and do not necessarily reflect the views of the National Science Foundation.

Abstract

This report presents an explicit, closed-form solution for the Green functions (displacements due to unit loads) corresponding to dynamic loads acting on (or within) layered strata. These functions embody all the essential mechanical properties of the medium, and can be used to derive solutions to problems of elastodynamics, such as scattering of waves by rigid inclusions, soil-structure interaction, seismic sources, etc. The solution is based on a discretization of the medium in the direction of layering, which results in a formulation yielding algebraic expressions whose integral transforms can readily be evaluated. The advantages of the procedure are: a) the speed and accuracy with which the functions can be evaluated (no numerical integration necessary); b) the potential application to problems of elastodynamics solved by the Boundary Integral Method, and c) the possibility of comparing and verifying numerical integral solutions implemented in computer codes.

The technique presented in this report is based on an Inversion of the Descent of Dimensions: that is, on a formulation of the solution to loads in the three-dimensional space using the solutions to the two-dimensional problems of horizontal, vertical and antiplane line loads. Some of the resulting expressions are similar to recent solutions reported by Tajimi (1980) and by Waas (1980), whose contributions came to the author's attention at the time this work was being completed.

Section 2 of this report presents the theory in detail, while section 3 is devoted to examples of application and comparison.

1 - INTRODUCTION

Interest in the solution to elastodynamic problems of continua subjected to static and dynamic loads is not new. as evidenced bv the well-known works of Kelvin (1848), Boussinesq (1878), Cerruti (1882), Lamb (1904), Mindlin (1936), and others. While these solutions have some theoretical appeal in themselves, they are really more important as tools in the solution of the involved boundary value problems arising in seismology and geomechanics. Despite the considerable work that has been done up to this date, however, the solutions available so far are restricted to solids of relatively simple geometry, such as full spaces, halfspaces, and homogeneous strata. The complexities introduced by layering are so formidable that only integral formulations that need to be evaluated numerically (Harkreider, 1964) are currently available. These complexities are obviated in this work by resorting to a discrete formulation, which is based on a linearization of the displacement field in the direction of layering. This technique has the advantage that the Green functions in the wave-number domain are algebraic rather than transcendental. Thus, the Hankel transforms required for an evaluation of the Green functions in the spatial domain can readily be computed in closed form.

2. THEORETICAL DERIVATION

2.1 Displacements and Stresses: Spatial vs. Wave-number Domain

The determination of the response of a soil deposit to dynamic loads, caused either by a seismic excitation or by prescribed forces at some location in the soil mass, falls mathematically into the area of wave-propagation theory. The formalism to study the propagation of waves in layered media was presented by Thomson (1959) and Haskell (1953) more than 25 years ago, and it is based on the use of transfer matrices in the frequency - wave-number domain. The solution technique for arbitrary loadings necessitates resolving the loads in terms of their temporal and spatial Fourier transforms, assuming them to be harmonic in time

and space. This corresponds formally to the use of the method of separation of variables to find solutions to the wave equation. Closed-form solutions are then found for simple cases by contour integration, while numerical solutions are needed for arbitrarily layered soils. The details of the procedures are well known, and need not be repeated here.

The first step in the computation for dynamic loads is then to find the harmonic displacements at the layer interfaces due to unit harmonic loads. In the transfer matrix approach, the (harmonic) displacements and internal stresses at a given interface define the state vector, which in turn is related through the transfer matrix to the state vectors at neighboring interfaces.

An alternative method of analysis for layered soils is the stiffness matrix approach presented by Kausel and Roesset (1981). In this procedure, the external loads applied at the layer interfaces are related to the displacements at these locations through stiffness matrices which are functions of both frequency and wavenumber. These stiffness matrices can be used and understood very much like those in structural analysis; in fact, standard techniques, such as substructuring, condensation, simultaneous solutions for multiple loadings, etc. are also applicable in this situation.

While the stiffness matrices presented in the above reference are valid for arbitrary layer thicknesses, frequency of excitation and wavenumber, their application is restricted either to the closed form solution of problems involving only simple geometries, or to numerical solutions for multilayered soils.

The formulation is intrinsically inefficient, because the transcendental functions which appear as arguments of the matrices makes the closed form evaluation of the integral transforms required for the analysis intractable in the general case.

If the layer thicknesses are small as compared to the wavelengths of interest (or if a finite layer is subdivided into several thin layers), it is possible to linearize the transcendental functions which govern

the displacements in the direction of layering. This procedure was first proposed by Lysmer and Waas (1972) and later generalized by Waas (1972) and Kausel (1974), although not in the context considered here. The method was also used by Drake (1972), to study alluvial valleys, while an extension to strata of finite width was given by Schlue (1979). Tassoulas (1981), on the other hand, employed this formulation to develop special macroelements (finite elements of large size) to study problems of geomechanics in layered soils. In principle, the technique is restricted to layered soils over rigid rock, although analyses of soils over elastic halfspaces could be accomplished with a hybrid formulation (i.e., taking the exact solution for the halfspace only). The principal advantage of the method is the substitution of algebraic expressions in place of the more involved transcendental functions. This concept will be applied in the following to study layered soils subjected to arbitrary dynamic loads.

Consider a layered soil system as shown in Fig. 1. The interfaces are dictated by discontinuities in material properties in the vertical direction, by the presence of external loads at a given elevation, or by restrictions on the thickness of layers as required by this discrete formulation. We define then the following stress and displacement vectors:

a) Cartesian coordinates:

$$\bar{S} = \begin{Bmatrix} \bar{\tau}_{xz} \\ \bar{\tau}_{yz} \\ i\bar{\sigma}_z \end{Bmatrix} \quad , \qquad \bar{u} = \begin{Bmatrix} \bar{u}_x \\ \bar{u}_y \\ i\bar{u}_z \end{Bmatrix} \tag{1}$$

in which $\bar{u}$, $\bar{\tau}$, $\bar{\sigma}$ are the displacement, shearing stress and normal stress components at a given elevation, in the direction identified by the subindex. The factor $i = \sqrt{-1}$ in front of $\bar{\sigma}_z$, $\bar{u}_z$ has the advantage that the stiffness matrices relating stresses and displacements thus defined are symmetric; for the static case, they are in addition real. The

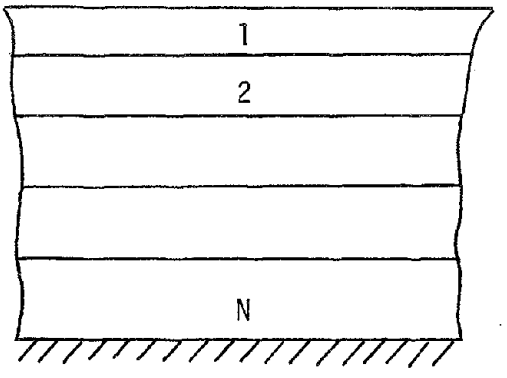

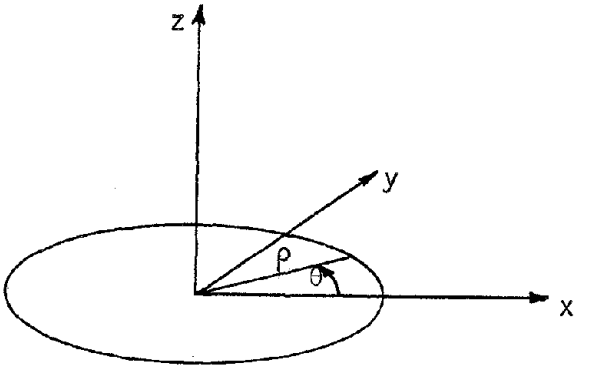

Figure 1

superscript bar, on the other hand, is a reminder that the components are functions of z only: that is, they are expressed in the transformed frequency - wave-number domain. The actual displacements and stresses at a point are obtained from the Fourier transform

$$\begin{Bmatrix} U \\ S \end{Bmatrix} = \frac{1}{(2\pi)^3} \iiint \begin{Bmatrix} \bar{U} \\ \bar{S} \end{Bmatrix} \exp i(\omega t - kx - \ell y)\, dk\, d\ell\, d\omega \quad , \tag{2}$$

in which ω = frequency of excitation, and k, ℓ are the wavenumbers. Since in the following developments only the solution for line loads are required to formulate the solution to point loads, we can set the second wavenumber equal to zero (ℓ=0). Also, the transformation in ω may be omitted, as we are interested only in harmonic solutions. Thus

$$\begin{Bmatrix} U \\ S \end{Bmatrix} = \frac{1}{2\pi} \int_{-\infty}^{\infty} \begin{Bmatrix} \bar{U} \\ \bar{S} \end{Bmatrix} e^{-ikx}\, dk \tag{3a}$$

and

$$\begin{Bmatrix} \bar{U} \\ \bar{S} \end{Bmatrix} = \int_{-\infty}^{\infty} \begin{Bmatrix} U \\ S \end{Bmatrix} e^{ikx}\, dx \quad , \tag{3b}$$

provided that the transformations exist.

b) Cylindrical coordinates:

The stress and displacement vectors are now:

$$\bar{S} = \begin{Bmatrix} \bar{\tau}_{\rho z} \\ \bar{\tau}_{\theta z} \\ \bar{\sigma}_z \end{Bmatrix} \quad , \qquad \bar{U} = \begin{Bmatrix} \bar{u}_\rho \\ \bar{u}_\theta \\ \bar{u}_z \end{Bmatrix} \quad . \tag{4}$$

with $\bar{u}$, $\bar{\tau}$, $\bar{\sigma}$ being again the displacement, tangential and normal stress components as identified by the subindices. Also, the superscript bar refers to the frequency - wave-number domain in cylindrical coordinates. Note the absence of the $i = \sqrt{-1}$ factor in front of $\bar{\sigma}_z$, $\bar{u}_z$, in contrast to the Cartesian case. The interrelationship with the spatial domain is now given by

$$U = \sum_{\mu=0}^{\infty} T_\mu \int_0^\infty k\, C_\mu\, \bar{U}\, dk \tag{5a}$$

and

$$\bar{U} = a_\mu \int_0^\infty \rho\, C_\mu \int_0^{2\pi} T_\mu\, U\, d\theta d\rho \tag{5b}$$

and similar expressions for S, $\bar{S}$. In these equations,

$$T_\mu = \text{diag}\,(\cos \mu\theta,\ -\sin \mu\theta,\ \cos \mu\theta) \tag{6a}$$

if the displacements (stresses) are symmetric with respect to the x axis, or

$$T_\mu = \text{diag}\,(\sin \mu\theta,\ \cos \mu\theta,\ \sin \mu\theta) \tag{6b}$$

if they are antisymmetric (nonsymmetric cases are combinations of these two situations). Also,

$$C_\mu = \begin{Bmatrix} \frac{d}{d(k\rho)} J_\mu & \frac{\mu}{k\rho} J_\mu & 0 \\ \frac{\mu}{k\rho} J_\mu & \frac{d}{d(k\rho)} J_\mu & 0 \\ 0 & 0 & -J_\mu \end{Bmatrix}, \tag{7}$$

in which $J_\mu = J_\mu(k\rho)$ are Bessel functions of the first kind and μ^{th} order. The orthogonalization factor a_μ is given by

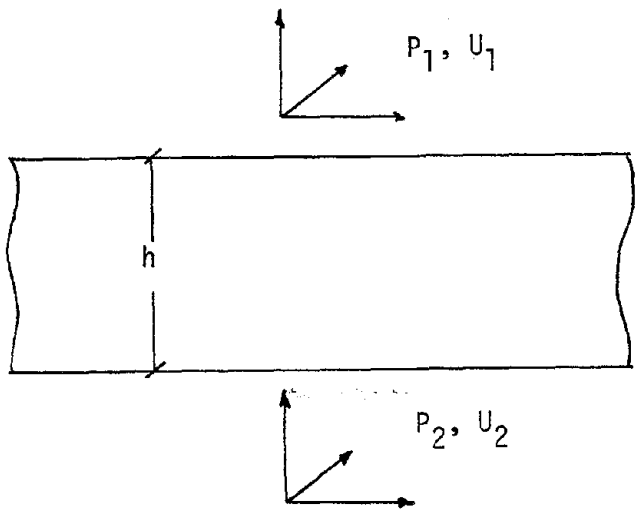

Fig. 2

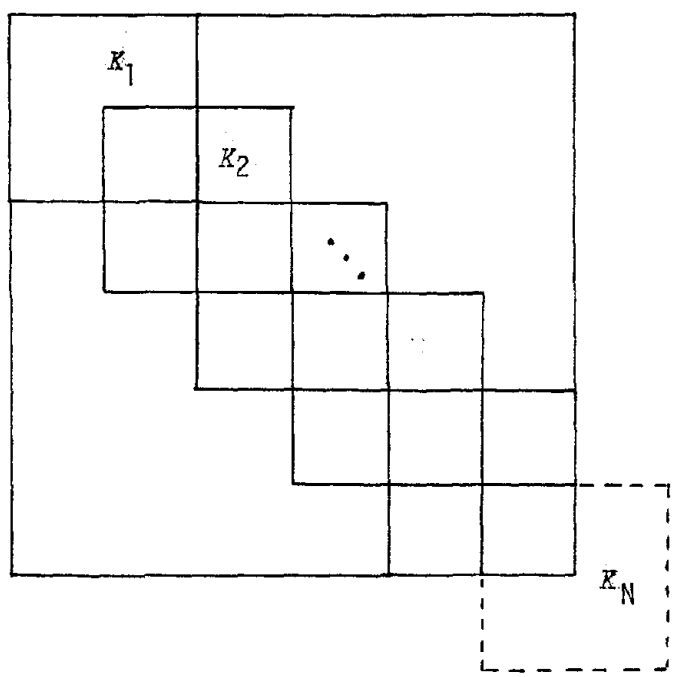

Fig. 3

$$\left.\begin{aligned} a_\mu &= \frac{1}{2\pi} \quad \text{if} \quad \mu=0 \\ &= \frac{1}{\pi} \quad \text{if} \quad \mu\neq 0 \end{aligned}\right\} \tag{8}$$

This corresponds to the well-known decomposition of the displacements and stresses in a Fourier series in the azimuthal direction, and cylindrical functions in the radial direction. The variation with time is given again by the factor exp $i\omega t$.

2.2 Stiffness Matrix Approach

Referring to Fig. 2, we isolate a specific layer and preserve equilibrium by application of external loads $\overline{P}_1 = \overline{S}_1$ at the upper interface, and $\overline{P}_2 = -\overline{S}_2$ at the lower interface. The relationship between forces (tractions) and displacements is then:

$$\begin{Bmatrix} \overline{P}_1 \\ \overline{P}_2 \end{Bmatrix} = \begin{Bmatrix} K_{11} & K_{12} \\ K_{21} & K_{22} \end{Bmatrix} \begin{Bmatrix} \overline{U}_1 \\ \overline{U}_2 \end{Bmatrix} \tag{9}$$

with

$$K_m = \begin{Bmatrix} K_{11} & K_{12} \\ K_{21} & K_{22} \end{Bmatrix} \tag{10}$$

being the (symmetric) stiffness matrix of the (m^{th}) layer under consideration. Explicit expressions for this matrix are given in Kausel and Roesset (1981).

In the case of a soil which consists of several layers, the global stiffness matrix $K = \{K_m\}$ is constructed by overlapping the contribution of the layer matrices at each "node" (interface) of the system (Fig. 3). The global load vector corresponds in this case to the prescribed external tractions at the interfaces. Thus, the assemblage and solution of the equations is formally analogous to the solution of structural dynamic problems in the frequency domain.

It is interesting to note that the stiffness matrix for cylindrical coordinates is identical to that of the plane strain (Cartesian) case, and is independent of the Fourier index μ. This implies, among other things, that the solution for point loads can be derived, in principle, from the solution for the three line load cases of the plane strain case; this is referred to as the inversion of the descent of dimensions, and forms the basis of the technique considered here. Thus, the load and displacement vectors $\overline{P}$, $\overline{U}$ in equation (9) may follow either from the cylindrical or the Cartesian formulation.

2.3 Thin Layer Formulation

In the case of thin layers, the layer stiffness matrix can be obtained as (Waas (1972), Kausel (1974), Kausel and Roesset (1981)).

$$K_m = A_m k^2 + B_m k + G_m - \omega^2 M_m \quad , \tag{11}$$

where k = wave number, ω = frequency of excitation; and A_m, B_m, G_m, M_m are the matrices given in Table 1 (which involve only material properties of the layers). In contrast to the continuum formulation, however, this discrete approach results in stiffness matrices that are algebraic rather than transcendental. Also, in this alternative, the displacements within the layer are obtained by linear interpolation between interfaces:

$$\overline{U} = \xi \overline{U}_1 + (1 - \xi)\, \overline{U}_2 \quad , \quad 0 \leq \xi \leq 1 \tag{12}$$

As in the continuum approach, the global stiffness matrix $K = \{K_m\}$ is obtained by overlapping the matrices for each layer (Fig. 3). In fact, the assemblage may be understood in the finite element sense, with each thin layer constituting a "linear" element. The global load and displacement vectors $\overline{P} = \{\overline{P}\}$, $\overline{U} = \{\overline{U}\}$ are then assembled with the "nodal" (interface) load and displacement vectors $\overline{P}$, $\overline{U}$. For prescribed loadings, $\overline{P}$, the displacements $\overline{U}$ are obtained by formal inversion of the stiffness matrix:

$$\overline{P} = K\, \overline{U} \tag{13a}$$

$$\overline{U} = K^{-1} \overline{P}. \tag{13b}$$

$$A_m = \frac{h}{6}\begin{Bmatrix} 2(\lambda+2G) & . & . & \lambda+2G & . & . \\ . & 2G & . & . & G & . \\ . & . & 2G & . & . & G \\ \lambda+2G & . & . & 2(\lambda+2G) & . & . \\ . & G & . & . & 2G & . \\ . & . & G & . & . & 2G \end{Bmatrix}$$

$$B_m = \frac{1}{2}\begin{Bmatrix} . & . & \lambda-G & . & . & -(\lambda+G) \\ . & . & . & . & . & . \\ \lambda-G & . & . & \lambda+G & . & . \\ . & . & \lambda+G & . & . & -(\lambda-G) \\ . & . & . & . & . & . \\ -(\lambda+G) & . & . & -(\lambda-G) & . & . \end{Bmatrix}$$

$$G_m = \frac{1}{h}\begin{Bmatrix} G & . & . & -G & . & . \\ . & G & . & . & -G & . \\ . & . & \lambda+2G & . & . & -(\lambda+2G) \\ -G & . & . & G & . & . \\ . & -G & . & . & G & . \\ . & . & -(\lambda+2G) & . & . & \lambda+2G \end{Bmatrix}$$

$$M_m = \frac{\rho h}{6}\begin{Bmatrix} 2 & . & . & 1 & . & . \\ . & 2 & . & . & 1 & . \\ . & . & 2 & . & . & 1 \\ 1 & . & . & 2 & . & . \\ . & 1 & . & . & 2 & . \\ . & . & 1 & . & . & 2 \end{Bmatrix}$$

λ = Lamé constant
G = shear modulus
ρ = mass density
h = layer thickness

} for soil with damping, use complex values.

$K = \{K_m\} = A\,k^2 + Bk + G - \omega^2 M$
$A = \{A_m\}$
$B = \{B_m\}$
$G = \{G_m\}$
$M = \{M_m\}$

TABLE 1

In practice, this inversion is not necessary, since either a Gaussian reduction would be employed, or the spectral decomposition described below could be used.

2.4 Spectral Decomposition of the Stiffness Matrix

The natural modes of wave propagation in the stratum are obtained from the eigenvalue problem that follows from setting the load vector equal to zero:

$$(A\ k_j^2 + B\ k_j + C)\ \phi_j = 0 \qquad (14)$$

with $C = G - \omega^2 M$. The notation for the displacement vector has been changed from $\bar{U}$ to ϕ_j to emphasize the identification as eigenvector. (The subindex j refers to the various possible solutions). Waas (1972) studied this problem in detail, although his notation and coordinate system were slightly different; his work was concerned with the development of a transmitting boundary (silent or absorbing boundary) for finite element models. Equation (14) constitutes a quadratic eigenvalue problem, with eigenvalues k_j and modal shapes ϕ_j.

This problem yields 6N eigenvalues k_j and eigenvectors, ϕ_j, with N being the total number of layers. 3N of these correspond to eigenvalues k_j, ϕ_j, while the other half correspond to eigenvalues $-k_j$, $\tilde{\phi}_j$ (with $\tilde{\phi}_j$ being obtained trivially from ϕ_j by reversing the sign of the vertical components). Following Waas, we choose the 3N modes that have eigenvalues k_j, whose imaginary part is negative if k_j is complex, or whose real part is positive if k_j is real. This implies selecting only the propagation modes that decay with distance to the source, or that propagate away from it.

While a quadratic eigenvalue problem can always be solved as a linear eigenvalue problem of double dimension, this is not necessary here because of the special structure of the matrices involved. To show this, we begin rearranging rows and columns by degrees of freedom rather than by interface (i.e., grouping first all horizontal, then all vertical, and finally all antiplane degrees of freedom). The resulting eigenvalue problem is then of the form

$$\begin{Bmatrix} k_j^2 A_x + C_x & k_j B_{xz} & \\ k_j B_{xz}^T & k_j^2 A_z + C_z & \\ & & k_j^2 A_y + C_y \end{Bmatrix} \begin{Bmatrix} \phi_{xj} \\ \phi_{zj} \\ \phi_{yj} \end{Bmatrix} = \begin{Bmatrix} 0 \\ 0 \\ 0 \end{Bmatrix} \tag{15}$$

with uncoupled antiplane mode ϕ_y. The matrices A_x, C_x, etc. are tri-diagonal and, except for B_{xz}, are symmetric. This eigenvalue problem may then be transformed into

$$\begin{Bmatrix} k_j^2 A_x + C_x & B_{xz} & \\ k_j^2 B_{xz}^T & k_j^2 A_z + C_z & \\ & & k_j^2 A_y + C_y \end{Bmatrix} \begin{Bmatrix} \phi_{xj} \\ k_j \phi_{zj} \\ \phi_{yj} \end{Bmatrix} = \begin{Bmatrix} 0 \\ 0 \\ 0 \end{Bmatrix} \tag{16}$$

which is a linear (although non-symmetric) eigenvalue problem in k^2. An alternative linear eigenvalue problem is also

$$\begin{Bmatrix} k_j^2 A_x + C_x & k_j^2 B_{xz} & \\ B_{xz}^T & k_j^2 A_z + C_z & \\ & & k_j^2 A_y + C_y \end{Bmatrix} \begin{Bmatrix} k_j \phi_{xj} \\ \phi_{zj} \\ \phi_{yj} \end{Bmatrix} = \begin{Bmatrix} 0 \\ 0 \\ 0 \end{Bmatrix} \tag{17}$$

having a characteristic matrix which is the transpose of that in Eq. (16).

Both of these eigenvalue problems yield the same eigenvalues and have associated "left" and "right" eigenvectors.

$$Y_j = \begin{Bmatrix} k_j \phi_{xj} \\ \phi_{zj} \\ \phi_{yj} \end{Bmatrix} \quad \text{and} \quad Z_j = \begin{Bmatrix} \phi_{xj} \\ k_j \phi_{zj} \\ \phi_{yj} \end{Bmatrix} \tag{18}$$

which are mutually orthogonal with respect to the characteristic equation (see below). Defining

$$\bar{A} = \begin{Bmatrix} A_x & & \\ B_{xz}^T & A_z & \\ & & A_y \end{Bmatrix} \qquad \bar{C} = \begin{Bmatrix} C_x & B_{xz} & \\ & C_z & \\ & & C_y \end{Bmatrix} \tag{18}$$

$$Y = \{Y_j\} \quad , \qquad Z = \{Z_j\} \qquad j = 1, 2, \ldots 3N$$

$$K = \text{diag}\{k_j\} = \begin{Bmatrix} K_R & \\ & K_L \end{Bmatrix} = \begin{Bmatrix} \text{"Rayleigh" modes} & \\ & \text{"Love" modes} \end{Bmatrix} \tag{19}$$

the eigenvalue problem may be written as

$$k_j^2 \bar{A} Z_j + \bar{C} Z_j = 0 \qquad \text{or} \qquad \bar{A} Z K^2 + \bar{C} Z = 0 \tag{20a}$$

and

$$k_j^2 \bar{A}^T Y_j + \bar{C}^T Y_j = 0 \qquad \text{or} \qquad \bar{A}^T Y K^2 + \bar{C}^T Y = 0 \tag{20b}$$

which satisfy the orthogonality conditions

$$\begin{aligned} Y_i^T \bar{A} Z_j &= 0 \quad \text{if } i \neq j \\ &\neq 0 \quad \text{if } i = j \end{aligned} \tag{21}$$

and a similar condition for $Y_i^T \bar{C} Z_j$. We choose here a normalization of the eigenvectors Y, Z which can be proved to be the same as the one used by Waas (see appendix):

$$Y^T \bar{A} Z = \begin{Bmatrix} K_R & \\ & I \end{Bmatrix} = N \tag{22a}$$

and by substitution into the eigenvalue problem,

$$\bar{Y}^T \bar{C} Z = -NK^2 \quad . \tag{22b}$$

Consider now the equilibrium equation in the wave-number domain (eq. 13a) (after rearranging columns and rows by d.o.f.'s).

$$(\overline{A}\, k^2 + \overline{C})\, \overline{U}^* = \overline{P}^* \tag{23}$$

with

$$\overline{U}^* = \begin{Bmatrix} \overline{U}_x \\ k\overline{U}_z \\ \overline{U}_y \end{Bmatrix} , \tag{24a}$$

$$\overline{P}^* = \begin{Bmatrix} \overline{P}_x \\ k\overline{P}_z \\ \overline{P}_y \end{Bmatrix} . \tag{24b}$$

Premultiplication by Y^T, and introducing $ZZ^{-1} = I$ yields

$$Y^T(\overline{A}\, k^2 + \overline{C})\, Z\, Z^{-1}\, \overline{U}^* = Y^T \overline{P}^* \tag{25}$$

and in view of eqs. (22) above

$$(Nk^2 - NK^2)\, Z^{-1}\, \overline{U}^* = Y^T\, \overline{P}^* \tag{26}$$

from which we can solve for $\overline{U}^*$:

$$\overline{U}^* = ZN^{-1}\, (Ik^2 - K^2)^{-1}\, Y^T \overline{P}^* \tag{27}$$

Since the in-plane eigenvalue problem is uncoupled from the antiplane problem, we can consider the two cases separately.

a) In-plane case

The reduced eivenvector is

$$Z = \{Z_j\} = \begin{Bmatrix} \{\phi_{xj}\} \\ \{\phi_{zj}\, k_j\} \end{Bmatrix} = \begin{Bmatrix} \Phi_x \\ \Phi_z\, K_R \end{Bmatrix} \tag{28a}$$

$$Y = \begin{Bmatrix} \Phi_X & K_R \\ \\ \Phi_Z & \end{Bmatrix} \tag{28b}$$

in which the spectral matrix K_R has 2N elements corresponding to the in-plane modes (the subscript R stands for Rayleigh).

From eqs. 27 we obtain, then

$$\begin{Bmatrix} \bar{U}_X \\ k\bar{U}_Z \end{Bmatrix} = \begin{Bmatrix} \Phi_X \\ \Phi_Z K_R \end{Bmatrix} \left(K_R k^2 - K_R^3 \right)^{-1} \begin{Bmatrix} K_R \Phi_X^T & \Phi_Z^T \end{Bmatrix} \begin{Bmatrix} \bar{\bar{P}}_X \\ k\bar{\bar{P}}_Z \end{Bmatrix} \tag{29}$$

yielding

$$\begin{Bmatrix} \bar{U}_X \\ \bar{U}_Z \end{Bmatrix} = \begin{Bmatrix} \Phi_X D_R \Phi_X^T & k\Phi_X K_R^{-1} D_R \Phi_Z^T \\ \\ \frac{1}{k} \Phi_Z K_R D_R \Phi_X^T & \Phi_Z D_R \Phi_Z^T \end{Bmatrix} \begin{Bmatrix} \bar{\bar{P}}_X \\ \\ \bar{\bar{P}}_Z \end{Bmatrix} \tag{30}$$

with
$$D_R = (k^2 I - K_R^2)^{-1} \tag{31}$$

(I being the identity matrix).

The matrix in front of the load vector in eq. (30) is the inverse of the global stiffness matrix, with rows and columns transposed so as to have first all horizontal and then all vertical degrees of freedom. Since this matrix is symmetric, so must its inverse be. Hence

$$k\, \Phi_X K_R^{-1} D_R \Phi_Z^T = \frac{1}{k} (\Phi_Z K_R D_R \Phi_X^T)^T = \frac{1}{k} \Phi_X D_R K_R \Phi_Z^T \tag{32}$$

Multiplying by k and combining the two sides,

$$\Phi_X (k^2 K_R^{-1} D_R - K_R D_R) \Phi_Z = \Phi_X K_R^{-1} (k^2 I - K_R^2) D_R \Phi_Z^T = 0 \tag{33}$$

but
$$k^2 I - K_R^2 = D_R^{-1} \quad ,$$

hence
$$\Phi_X K_R^{-1} \Phi_Z^T = 0 \tag{34}$$

(Observe that the matrices Φ_x, Φ_z are rectangular, not square). This relationship could also have been proved starting with an alternate form of equation (22), namely,

$$(\overline{A}^T k^2 + \overline{C}^T)\overline{U}^{**} = \overline{P}^{**} \tag{35}$$

with

$$\overline{U}^{**} = \begin{Bmatrix} \overline{U}_x\, k \\ \overline{U}_z \end{Bmatrix}, \qquad \overline{P}^{**} = \begin{Bmatrix} \overline{P}_x\, k \\ \overline{P}_z \end{Bmatrix} \tag{36}$$

and using again the orthogonality condition. Thus equation (30) transforms into

$$\begin{Bmatrix} \overline{U}_x \\ \overline{U}_z \end{Bmatrix} = \begin{bmatrix} \Phi_x D_R \Phi_x^T & k\, \Phi_x K_R^{-1} D_R \Phi_z^T \\ k\, \Phi_z D_R K_R^{-1} \Phi_x^T & \Phi_z D_R \Phi_z^T \end{bmatrix} \begin{Bmatrix} \overline{P}_x \\ \overline{P}_z \end{Bmatrix} \tag{37}$$

and we have an explicit expression (in terms of k) for the in-plane flexibility matrix (inverse of the stiffness matrix, with rows/columns transposed to accommodate the new order of degrees of freedom).

b) Antiplane case:

Following a procedure which is entirely analogous to the in-plane case, one obtains

$$\overline{U}_y = \Phi_y D_L \Phi_y^T \overline{P}_y \tag{38}$$

$$\text{with} \qquad D_L = (k^2 I - K_L^2)^{-1} \tag{39}$$

in which K_L = diag (k_j) has only N elements, corresponding to the antiplane modes. The subscript L refers to the Love modes.

2.5 Green Functions for Line Loads

A unit line load is described in the spatial domain by an expression of the form

$$\tau = \delta(x-x_o) \tag{40}$$

which is prescribed at a given elevation z_o, with abscissa x_o. τ is either a normal or shearing traction, and δ is the Dirac Delta function. The Fourier transform for a load applied in the vertical plane passing through the origin ($x_o = 0$) is

$$\bar{\tau} = \int_{-\infty}^{\infty} \delta(x) e^{ikx}\, dx = 1 \tag{41}$$

which is independent of the wavenumber k. Thus, the load vectors in Eqs. (37) or (38) have a single non-zero unit element in the row that corresponds to the elevation and direction of the applied line load. To consider the general case of loads applied at any elevation and direction, we replace the load vectors in these equations by identity matrices; determination of the Green functions requires then a Fourier transformation of the flexibility matrices. This necessitates evaluation of the following integrals:

$$\frac{1}{2\pi}\int_{-\infty}^{\infty} D\, e^{-ikx}\, dk \quad \text{and} \quad \frac{1}{2\pi}\int_{-\infty}^{\infty} k\, D\, e^{-ikx}\, dk \tag{42}$$

with $D = \text{diag}\,(k^2 - k_j^2)^{-1}$. Each of the diagonal terms is then of the form

$$I_1 = \frac{1}{2\pi}\int_{-\infty}^{\infty} \frac{e^{-ikx}}{k^2 - k_j^2}\, dk \qquad I_m(k_j) < 0$$

$$= \frac{1}{2ik_j} e^{-ik_j x} \qquad x \geq 0$$

$$= \frac{1}{2ik_j} e^{ik_j x} \qquad x \leq 0 \tag{43}$$

$$I_2 = \frac{1}{2\pi}\int_{-\infty}^{\infty} \frac{k\, e^{-ikx}}{k^2 - k_j^2}\, dk \qquad I_m(k_j) < 0$$

$$= \frac{1}{2i}\, e^{-ik_j x} \qquad x > 0$$

$$= 0 \quad (P.V.) \qquad x = 0$$

$$= -\frac{1}{2i}\, e^{ik_j x} \qquad x < 0 \tag{44}$$

Defining

$$E_x = \text{diag}\left\{e^{-ik_j x}\right\} = \begin{Bmatrix} E_x^R & \\ & E_x^L \end{Bmatrix} \tag{45}$$

the integrals in (42) can then be expressed as

$$\frac{1}{2\pi}\int_{-\infty}^{\infty} D\, e^{-ikx}\, dk = \frac{1}{2i}\, E_{|x|} K^{-1} \tag{46a}$$

$$\frac{1}{2\pi}\int_{-\infty}^{\infty} k\, D\, e^{-ikx}\, dk = \begin{cases} \frac{1}{2i}\, E_x & x > 0 \\ 0 & x = 0 \\ -\frac{1}{2i}\, E_{-x} & x < 0 \end{cases} \tag{46b}$$

a) <u>In-plane line loads</u>

For the in-plane case, the Green functions are then obtained from Eqs. (37), (46) as

$$\begin{Bmatrix} U_x \\ U_z \end{Bmatrix} = \frac{1}{2i} \begin{Bmatrix} \Phi_x\, E^R_{|x|}\, K_R^{-1}\, \Phi_x^T & \pm\Phi_x\, E^R_{|x|}\, K_R^{-1}\, \Phi_z^T \\ \pm\Phi_z\, K_R^{-1}\, E^R_{|x|}\, \Phi_x^T & \Phi_z\, E^R_{|x|}\, K_R^{-1}\, \Phi_z^T \end{Bmatrix} \tag{47}$$

in which the positive sign is chosen for $x \geq 0$, and the negative sign for $x < 0$. The special case $x = 0$ is included in the above equation because when $E^R_{x=0} = I$, the off-diagonal submatrix reduces to Eq. (34),

(which is zero). The superscript R in E_x^R refers again to the submatrix of E_x that corresponds to the in-plane (Rayleigh) modes.

It is important to note that the components of the vertical (unit) load vector and the vertical displacement vector carry an implicit factor $i = \sqrt{-1}$ (see Eq. (1)). Consideration of this factor affects the coupling terms only; the true horizontal displacements due to vertical loads are $\pm \frac{1}{2} \Phi_x \, E^R_{|x|} \, K_R^{-1} \, \Phi_z^T$, while the vertical displacements due to horizontal loads are $\mp \frac{1}{2} \Phi_z \, K_R^{-1} \, E^R_x \, \Phi_x^T$.

For x = 0, the right-hand side of Eq. (47) represents the inverse of the stiffness matrix of two Waas-Lysmer transmitting boundaries joined at the origin of coordinates (one transmitting boundary for the right layers, the other for the left layers.)

b) Antiplane case

Using Eqs. (38) and (46a), one obtains

$$U_y = \frac{1}{2i} \Phi_y \, E^L_{|x|} \, K_L^{-1} \, \Phi_y^T \tag{48}$$

in which E_x^L is the submatrix of E_x corresponding to the antiplane (Love) modes. Again, the right-hand side is the inverse of two antiplane transmitting boundaries when x = 0.

2.6 Green Functions in Cylindrical Coordinates

2.6.1 Preliminary definitions

Consider once more the flexibility matrices in Eqs. (37) and (38), obtained for the plane strain cases. We define then the N x N matrices

$$F_{xx} = \left\{ f_{xx} \right\} = \Phi_x \, D_R \, \Phi_x^T$$

$$F_{xz} = \left\{ f_{xz} \right\} = k \, \Phi_x \, K_R^{-1} \, D_R \, \Phi_z^T$$

$$F_{zx} = \left\{ f_{zx} \right\} = k \, \Phi_z \, D_R \, K_R^{-1} \, \Phi_x^T = F_{xz}^T$$

$$F_{zz} = \left\{f_{zz}\right\} = \Phi_z \, D_R \, \Phi_z^T$$

$$F_{yy} = \left\{f_{yy}\right\} = \Phi_y \, D_L \, \Phi_y^T \qquad (49)$$

Also

$$\Phi_x = \left\{\phi_x^{m\ell}\right\} \qquad m = 1, \ldots N; \quad \ell = 1, \ldots 2N$$

$$\Phi_z = \left\{\phi_z^{m\ell}\right\} \qquad m = 1, \ldots N; \quad \ell = 1, \ldots 2N$$

$$\Phi_y = \left\{\phi_y^{m\ell}\right\} \qquad m = 1, \ldots N; \quad \ell = 1, \ldots N \; . \qquad (50)$$

The elements of the flexibility matrix are then

$$f_{xx} = \sum_{\ell=1}^{2N} \phi_x^{m\ell} \, \phi_x^{n\ell} \, a_\ell^R \qquad (51a)$$

$$f_{xz} = \sum_{\ell=1}^{2N} \phi_x^{m\ell} \, \phi_z^{n\ell} \, b_\ell^R = \sum_{\ell=1}^{2N} c_\ell \, \phi_x^{m\ell} \, \phi_z^{n\ell} \qquad (51b)$$

$$f_{zx} = \sum_{\ell=1}^{2N} \phi_z^{m\ell} \, \phi_x^{n\ell} \, b_\ell^R = \sum_{\ell=1}^{2N} c_\ell \, \phi_z^{m\ell} \, \phi_x^{n\ell} \qquad (51c)$$

$$f_{zz} = \sum_{\ell=1}^{2N} \phi_z^{m\ell} \, \phi_z^{n\ell} \, a_\ell^R \qquad (51d)$$

$$f_{yy} = \sum_{\ell=1}^{N} \phi_y^{m\ell} \, \phi_y^{n\ell} \, a_\ell^L \qquad (51e)$$

in which

$$a_\ell = \frac{1}{k^2 - k_\ell^2} \quad , \quad b_\ell = \frac{k}{k_\ell (k^2 - k_\ell^2)} \quad , \quad c_\ell = \frac{k_\ell}{k} \frac{1}{(k^2 - k_\ell^2)} \qquad (52)$$

(The superscripts R, L in a_ℓ, b_ℓ indicate the use of the Rayleigh/Love wavenumbers $k_\ell = k_\ell^R$ or $k_\ell = k_\ell^L$). The equivalence in (51b), (51c) is due to Eqs. (32) and (34).

The flexibility coefficients (displacements) at the m^{th} elevation due to loads at the n^{th} elevation are then

$$F = \begin{Bmatrix} f_{xx} & 0 & f_{xz} \\ 0 & f_{yy} & 0 \\ f_{zx} & 0 & f_{zz} \end{Bmatrix} \tag{53}$$

which shall be used in the following sections.

2.6.2 Green functions for disk loads

a) Horizontal disk load:

Referring to fig. 4a, the components in cylindrical coordinates of a uniform load q distributed over a disk of radius R is

$$P = q \begin{Bmatrix} \cos\theta \\ -\sin\theta \\ 0 \end{Bmatrix}, \qquad 0 \leq \rho < R \tag{54}$$

Using Eq. (5b)(replacing U by P) to express these functions in the wavenumber domain, we obtain first

$$\int_0^{2\pi} T_\mu P \, d\theta = q \int_0^{2\pi} \begin{Bmatrix} \cos\mu\theta & \cos\theta \\ \sin\mu\theta & \sin\theta \\ 0 \end{Bmatrix} d\theta = \pi q \begin{Bmatrix} 1 \\ 1 \\ 0 \end{Bmatrix} \quad \text{if } \mu = 1 \tag{55}$$

$$= 0 \qquad \text{if } \mu \neq 1.$$

so that (with $\mu = 1$, and $J_1' = dJ_1/dk\rho$):

$$\overline{P} = \frac{1}{\pi} \pi q \int_0^R \rho C_1 \begin{Bmatrix} 1 \\ 1 \\ 0 \end{Bmatrix} d\rho \qquad (C_1 = C_{\mu=1}, \text{ see Eq. (7)})$$

$$= q \int_0^R \rho \begin{Bmatrix} J_1' & \frac{1}{k\rho} J_1 & \\ \frac{1}{k\rho} J_1 & J_1' & \\ & & -J_1 \end{Bmatrix} \begin{Bmatrix} 1 \\ 1 \\ 0 \end{Bmatrix} d\rho$$

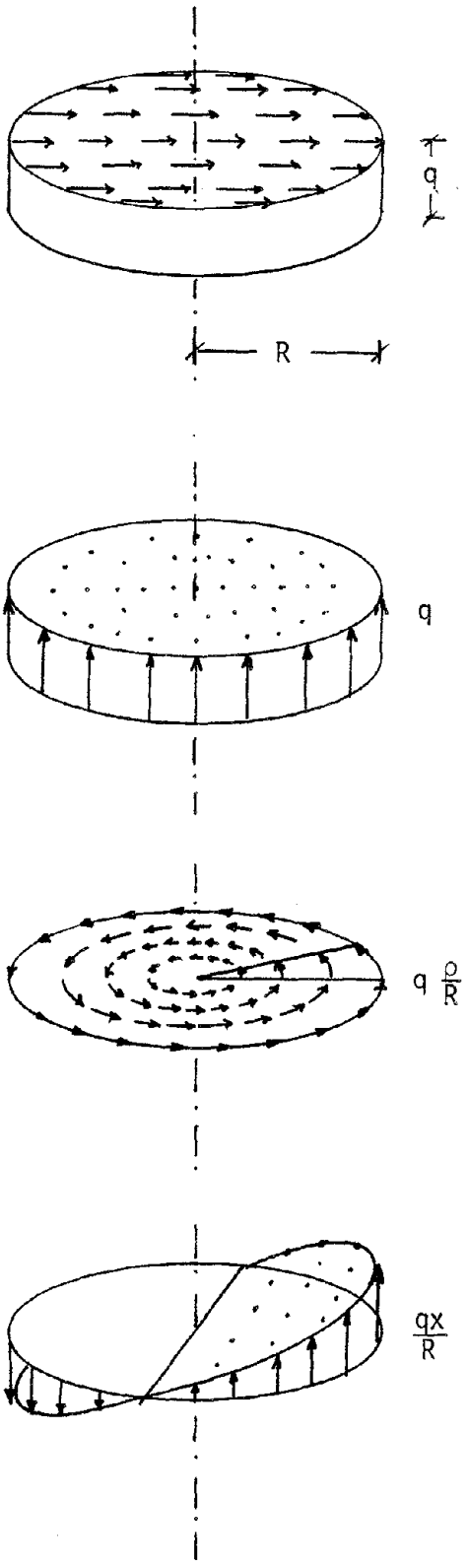

a) horizontal disk load
($P_x = \pi R^2 q$)

b) vertical disk load
($P_z = \pi R^2 q$)

c) torsional disk load
($M_t = \frac{\pi R^3}{2} q$)

d) rocking disk load
($M_r = \frac{\pi R^3}{4} q$)

Fig. 4

$$\overline{P} = q \int_0^R \rho\, J_0(k\rho)d\rho \begin{Bmatrix} 1 \\ 1 \\ 0 \end{Bmatrix}$$

$$= q \begin{Bmatrix} 1 \\ 1 \\ 0 \end{Bmatrix} \frac{R}{k} J_1 (kR) \tag{56}$$

If the disk load is applied at the n^{th} elevation, the resulting displacements at the m^{th} elevation in the wavenumber domain are

$$\overline{U} = F\, \overline{P} \tag{57}$$

with F being given by Eq. (53). The displacements in the spatial domain follow then from Eq. (5a):

$$U = T_1 \int_0^\infty k\, C_1\, \overline{U}\, dk \tag{58}$$

Substituting (53), (56), and (57), we obtain

$$U = q\, R\, T_1 \int_0^\infty C_1 \begin{Bmatrix} f_{xx} \\ f_{yy} \\ f_{zx} \end{Bmatrix} J_1(kR)dk \quad (C_1 = C_{\mu=1}, \text{ see Eq. (7)})$$

$$= q\, R\, T_1 \left[\int_0^\infty \begin{Bmatrix} f_{xx} & J_0(k\rho)\, J_1(kR) \\ f_{yy} & J_0(k\rho)\, J_1(kR) \\ -f_{zx} & J_1(k\rho)\, J_1(kR) \end{Bmatrix} dk + \right.$$

$$\left. + \frac{1}{\rho} \int_0^\infty \frac{1}{k} \begin{Bmatrix} f_{yy} - f_{xx} \\ f_{xx} - f_{yy} \\ 0 \end{Bmatrix} J_1(k\rho)J_1(kR)\, dk \right] \tag{59}$$

Evaluation of the above expression requires the following integrals (because of the factors a_ℓ, b_ℓ in Eqs. (51))

$$I_{1\ell} = \int_0^\infty \frac{1}{k^2 - k_\ell^2} J_0(k\rho)\, J_1(kR)\, dk \qquad (60a)$$

$$I_{2\ell} = \int_0^\infty \frac{k}{k^2 - k_\ell^2} J_1(k\rho)\, J_1(kR)\, dk \qquad (60b)$$

$$I_{3\ell} = \int_0^\infty \frac{1}{k(k^2 - k_\ell^2)} J_1(k\rho)\, J_1(kR)\, dk \qquad (60c)$$

These integrals are given in Table 2.

Substituting Eqs (51) into (Eq. 59), and considering the above integrals, we obtain for the displacements at the m^{th} interface due to a disk load at the n^{th} interface: (T_1 is defined by Eq. (6a))

$$u_\rho = qR \left[\sum_{\ell=1}^{2N} \phi_x^{m\ell} \phi_x^{n\ell} \frac{d}{d\rho} I_{3\ell}^R + \frac{1}{\rho} \sum_{\ell=1}^{N} \phi_y^{m\ell} \phi_y^{n\ell} I_{3\ell}^L\right] (\cos\theta) \qquad (61a)$$

$$u_\theta = qR \left[\frac{1}{\rho} \sum_{\ell=1}^{2N} \phi_x^{m\ell} \phi_x^{n\ell} I_{3\ell}^R + \sum_{\ell=1}^{N} \phi_y^{m\ell} \phi_y^{n\ell} \frac{d}{d\rho} I_{3\ell}^L\right] (-\sin\theta) \qquad (61b)$$

$$u_z = -qR \left[\sum_{\ell=1}^{2N} \phi_z^{m\ell} \phi_x^{n\ell} I_{3\ell}^R \; k_\ell^R\right] (\cos\theta) \qquad (61c)$$

in which again the superscript R, L in the functions $I_{j\ell}$ refer to the in-plane and antiplane wavenumbers k_ℓ^R, k_ℓ^L used as arguments. Also, $\frac{d}{d\rho} I_3 = I_1 - \frac{1}{\rho} I_3$. Note that $\lim_{\rho \to 0} I_{3\ell}/\rho$ exists, since $\lim_{z \to 0} J_1(z)/z = 1/2$.

The average horizontal displacement under the disk load can also be derived from the above expression. Since

$$u_x = u_\rho \cos\theta - u_\theta \sin\theta$$

$$= \tilde{u} \cos^2\theta + \tilde{v} \sin^2\theta \qquad (62)$$

in which $\tilde{u}$, $\tilde{v}$ are the amplitudes of u_ρ, u_θ in Eq. (61) above (i.e., omitting the factors $\cos\theta$, $-\sin\theta$), it follows that

Table 2

$$I_{1\ell} = \int_0^\infty \frac{1}{k^2-k_\ell^2} J_0(k\rho)\, J_1(kR)dk = \quad I_m(k_\ell) < 0$$

$$I^*_{1\ell}(\rho,R) = I_{1\ell}(R,\rho)$$

$$\begin{cases} \frac{\pi}{2ik_\ell} J_0(k_\ell\rho)\, H_1^{(2)}(k_\ell R) - \frac{1}{Rk_\ell^2} & 0 \le \rho \le R \\ \frac{\pi}{2ik_\ell} J_1(k_\ell R)\, H_0^{(2)}(k_\ell\rho) & R \le \rho \end{cases}$$

$$I_{2\ell} = \int_0^\infty \frac{k}{k^2-k_\ell^2} J_1(k\rho)\, J_1(kR)dk = \quad Im(k_\ell) < 0$$

$$\begin{cases} \frac{\pi}{2i} J_1(k_\ell\rho)\, H_1^{(2)}(k_\ell R) & 0 \le \rho < R \\ \frac{\pi}{2i} J_1(k_\ell R)\, H_1^{(2)}(k_\ell\rho) & R \le \rho \end{cases}$$

$$I_{3\ell} = \int_0^\infty \frac{1}{k(k^2-k_\ell^2)} J_1(k\rho)\, J_1(kR)dk = \quad Im(k_\ell) < 0$$

$$\begin{cases} \frac{\pi}{2ik_\ell^2} J_1(k_\ell\rho)\, H_1^{(2)}(k_\ell R) - \frac{\rho}{2Rk_\ell^2} & 0 \le \rho \le R \\ \frac{\pi}{2ik_\ell^2} J_1(k_\ell R)\, H_1^{(2)}(k_\ell\rho) - \frac{R}{2\rho k_\ell^2} & R \le \rho \end{cases}$$

$$I_{4\ell} = \int_0^\infty \frac{k}{k^2-k_\ell^2} J_0(k\rho)\, J_0(kR)dk = \quad Im(k_\ell) < 0$$

$$\begin{cases} \frac{\pi}{2i} J_0(k_\ell\rho)\, H_0^{(2)}(k_\ell R) & 0 \le \rho \le R \\ \frac{\pi}{2i} J_0(k_\ell R)\, H_0^{(2)}(k_\ell\rho) & R \le \rho \end{cases}$$

Note: $I_{2\ell} = -\frac{dI_{1\ell}}{d\rho}$; $I_{1\ell} = \frac{1}{\rho} I_{3\ell} + \frac{d}{d\rho} I_{3\ell}$; $I_{4\ell} = \frac{1}{R} I_{1\ell} + \frac{d}{dR} I_{1\ell} = \frac{1}{\rho} I^*_{1\ell} + \frac{d}{d\rho} I^*_{1\ell}$

$$u_{x(\text{average})} = \frac{1}{\pi R^2} \int_0^R \int_0^{2\pi} u_x \rho \, d\rho \, d\theta$$

$$= \frac{1}{R^2} \int_0^R (\tilde{u} + \tilde{v}) \rho \, d\rho \tag{63}$$

Since $\frac{dI_3}{d\rho} = I_1 - \frac{1}{\rho} I_3$, evaluation of the above equation requires the integral

$$\bar{I}_{1\ell} = \frac{1}{R^2} \int_0^R I_{1\ell} \, \rho \, d\rho$$

$$= \frac{1}{R^2} \int_0^R \rho \int_0^\infty \frac{1}{k^2 - k_\ell^2} J_0(k\rho) \, J_1(kR) \, dk \, d\rho$$

$$= \frac{1}{R^2} \int_0^\infty \frac{J_1(kR)}{k^2 - k_\ell^2} \int_0^R \rho \, J_0(k\rho) \, d\rho \, dk$$

$$= \frac{1}{R} \int_0^\infty \frac{J_1^2(kR)}{k(k^2 - k_\ell^2)} \, dk$$

$$= \frac{1}{R} I_{3\ell} \Big|_{\rho=R} \tag{64}$$

We notice also that addition of (61a) and (61b) (without the factors cos θ, -sin θ) cancels the terms in $I_{3\ell}$. Hence

$$u_{x(\text{average})} = q \left[\sum_{\ell=1}^{2N} \phi_x^{m\ell} \, \phi_x^{n\ell} \, I_{3\ell}^R + \sum_{\ell=1}^{N} \phi_y^{m\ell} \, \phi_y^{n\ell} \, I_{3\ell}^L \right] \Big|_{\rho=R} \tag{65}$$

b) Vertical disk load

The load vector in the spatial domain is (Fig. 4b)

$$P = q \begin{Bmatrix} 0 \\ 0 \\ 1 \end{Bmatrix} , \qquad 0 \leq \rho \leq R \tag{66}$$

Using Eq. (5b) to express this vector in the wavenumber domain, we obtain

$$\begin{aligned} \overline{P} &= a_\mu \int_0^\infty \int_0^{2\pi} \rho C_\mu T_\mu P \, d\theta \, d\rho \\ &= a_\mu q \int_0^R \rho C_\mu \int_0^{2\pi} \begin{Bmatrix} 0 \\ 0 \\ \cos \mu\theta \end{Bmatrix} d\theta \, d\rho \\ &= \begin{cases} q \int_0^R \rho C_0 \begin{Bmatrix} 0 \\ 0 \\ 1 \end{Bmatrix} d\rho = \frac{qR}{k} J_1(kR) \begin{Bmatrix} 0 \\ 0 \\ -1 \end{Bmatrix} & \text{for } \mu = 0 \\ 0 & \mu \neq 0 \end{cases} \end{aligned} \tag{67}$$

The displacements at the m^{th} elevation due to a vertical disk load at the n^{th} elevation are then

$$U = T_0 \int_0^\infty k \, C_0 \, \overline{U} \, dk , \qquad \overline{U} = F \, \overline{P} \tag{68}$$

Substituting (53) and (67), we obtain

$$\begin{aligned} U &= qR \, T_0 \int_0^\infty C_0 \begin{Bmatrix} -f_{xz} \\ 0 \\ -f_{zz} \end{Bmatrix} J_1 (kR) \, dk \\ &= qR \, T_0 \int_0^\infty \begin{Bmatrix} f_{xz} \, J_1 (k\rho) \, J_1(kR) \\ 0 \\ f_{zz} \, J_0 (k\rho) \, J_0(kR) \end{Bmatrix} dk \end{aligned} \tag{69}$$

Substituting Eqs. (51) into Eq. (69) and considering Eqs. (60), we obtain

$$u_\rho = qR \sum_{\ell=1}^{2N} \phi_x^{m\ell} \phi_z^{n\ell} I_{2\ell}^R / k_\ell \tag{70a}$$

$$u_\theta = 0 \tag{70b}$$

$$u_z = qR \sum_{\ell=1}^{2N} \phi_z^{m\ell} \phi_z^{n\ell} I_{1\ell}^R \tag{70c}$$

The average vertical displacement under the disk load is

$$u_{z(\text{average})} = \frac{1}{\pi R^2} \int_0^R \int_0^{2\pi} u_z \rho \, d\rho \, d\theta$$

$$= \frac{2}{R^2} \int_0^R u_z \rho \, d\rho \tag{71}$$

and in view of Eqs. (64, 70c)

$$u_{z(\text{average})} = 2q \sum_{\ell=1}^{2N} \phi_z^{m\ell} \phi_z^{n\ell} I_{3\ell}^R \Big|_{\rho=R} \tag{72}$$

c) Torsional disk load

The steps are the same as for the previous two cases; it suffices then to give the essential results only.

Load vector in spatial domain (Fig. 4c):

$$P = q \frac{\rho}{R} \begin{Bmatrix} 0 \\ 1 \\ 0 \end{Bmatrix} \tag{73}$$

Load vector in wavenumber domain ($\mu = 0$):

$$\overline{P} = \frac{qR}{k} [J_0(kR) - \frac{2}{kR} J_1(kR)] \begin{Bmatrix} 0 \\ 1 \\ 0 \end{Bmatrix} \tag{74}$$

Displacement integral:

$$U = qR \int_o^\infty C_o \begin{Bmatrix} 0 \\ f_{yy} \\ 0 \end{Bmatrix} [J_o(kR) - \frac{2}{kR} J_1(kR)]dk \tag{75}$$

Displacements:

$$u_\rho = 0 \tag{76a}$$

$$u_\theta = qR \sum_{\ell=1}^{N} \phi_y^{m\ell} \phi_y^{n\ell} (\frac{2}{R} I_{3\ell}^{L} - I_{1\ell}^{*L}) \tag{76b}$$

$$u_z = 0 \tag{76c}$$

in which $I_{1\ell}^{*}$ is the same as $I_{1\ell}$, but interchanging ρ by R (see Table 2).

d) Rocking (moment) disk load:

Following the same steps as before, we obtain the following results:

Load vector in spatial domain (Fig. 4d):

$$P = \begin{Bmatrix} 0 \\ 0 \\ 1 \end{Bmatrix} q \frac{\rho}{R} \cos\theta \tag{77}$$

Load vector in wavenumber domain: ($\mu = 1$)

$$\bar{P} = \begin{Bmatrix} 0 \\ 0 \\ -1 \end{Bmatrix} [\frac{2}{kR} J_1(kR) - J_o(kR)] \frac{qR}{k} \tag{78}$$

Displacement integral

$$U = q\, R\, T_1 \int_o^\infty C_1 \begin{Bmatrix} -f_{xz} \\ 0 \\ -f_{zz} \end{Bmatrix} [\frac{2}{kR} J_1(kR) - J_o(kR)]\, dk \tag{79}$$

Displacements:

$$u_\rho = qR \left[\sum_{\ell=1}^{2N} \phi_x^{m\ell} \phi_z^{n\ell} \left(- \frac{2}{R} I_{1\ell}^R - \frac{1}{\rho} I_{1\ell}^{*R} + \frac{2}{\rho R} I_{3\ell}^R + I_{4\ell}^R\right)/k_\ell \right] (\cos \theta)$$

$$= qR \left[\sum_{\ell=1}^{2N} \phi_x^{m\ell} \phi_z^{n\ell} \frac{d}{d\rho} \left(I_{1\ell}^{*R} - \frac{2}{R} I_{3\ell}^R\right)/k_\ell \right] (\cos \theta)$$

$$u_\theta = qR \left[\sum_{\ell=1}^{2N} \phi_x^{m\ell} \phi_z^{n\ell} \frac{1}{\rho} \left(I_{1\ell}^{*R} - \frac{2}{R} I_{3\ell}^R\right)/k_\ell \right] (-\sin \theta)$$

$$u_z = qR \left[\sum_{\ell=1}^{2N} \phi_z^{m\ell} \phi_z^{n\ell} \left(\frac{2}{R} I_{3\ell}^R - I_{1\ell}^{*R}\right) \right] (\cos \theta) \qquad (20)$$

2.6.3 Green functions for ring loads

These functions can be obtained from the previous results for disk loads by simple algebraic manipulations. If $G(\rho, r)$ represents the Green function at a circle having radius ρ due to a unit ring load with radius r, then the Green functions for disk loads having radius R follow from the convolution integral

$$g(\rho, R) = \int_0^R G(\rho, r)\, q(r) dr \qquad (81)$$

in which $q(r)$ is the intensity of the ring load. Taking derivative with respect to R, we obtain

$$\frac{\partial g}{\partial R} = G(\rho, R)\, q(R) \qquad (82)$$

Hence

$$G(\rho, R) = \frac{1}{q(R)} \frac{\partial g(\rho, R)}{\partial R} \qquad (83)$$

The Green functions for ring loads are then simply the derivative with respect to R of the Green functions for disk loads. Since this operation is straightforward, only the final results will be given below.

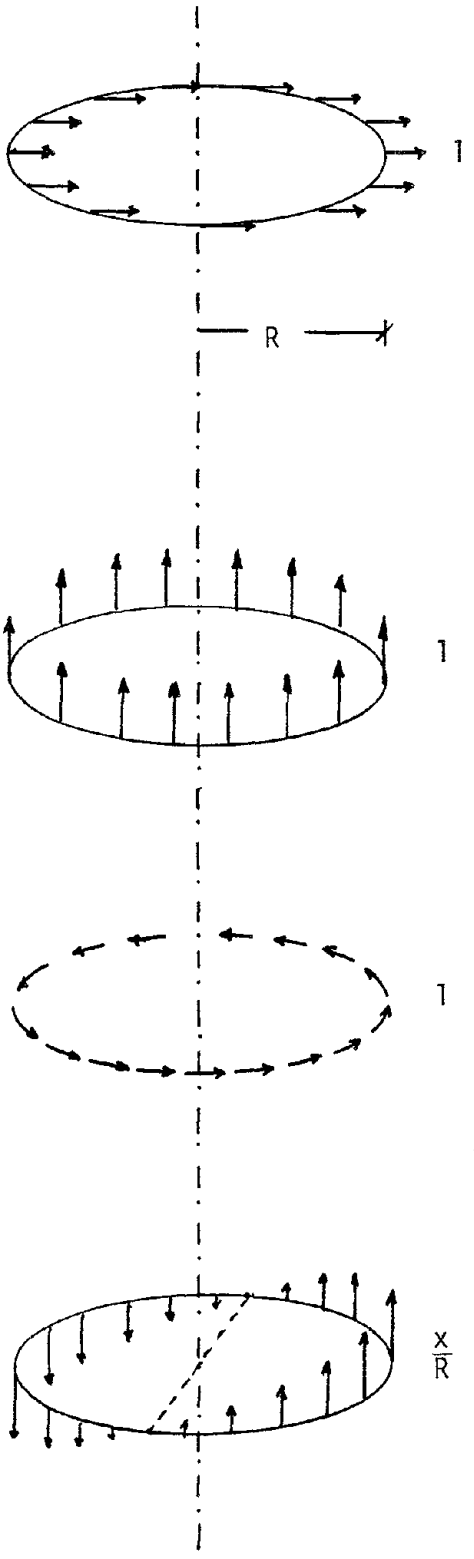

a) horizontal ring load
($P_x = 2\pi R$)

b) vertical ring load
($P_z = 2\pi R$)

c) torsional ring load
($M_t = 2\pi R^2$)

d) rocking ring load
($M_r = \pi R^2$)

Fig. 5

a) Horizontal ring load. (Fig. 5a):

$$u_\rho = R \left[\sum_{\ell=1}^{2N} \phi_x^{m\ell} \phi_x^{n\ell} \frac{d}{d\rho} I_{1\ell}^{*R} + \frac{1}{\rho} \sum_{\ell=1}^{N} \phi_y^{m\ell} \phi_y^{n\ell} I_{1\ell}^{*L} \right] (\cos \theta) \tag{84a}$$

$$u_\theta = R \left[\frac{1}{\rho} \sum_{\ell=1}^{2N} \phi_x^{m\ell} \phi_x^{n\ell} I_{1\ell}^{*R} + \sum_{\ell=1}^{N} \phi_y^{m\ell} \phi_y^{n\ell} \frac{d}{d\rho} I_{1\ell}^{*L} \right] (-\sin \theta) \tag{84b}$$

$$u_z = R \left[\sum_{\ell=1}^{2N} \phi_z^{m\ell} \phi_x^{n\ell} (- I_{1\ell}^{*} k_\ell) \right] (\cos \theta) \tag{84c}$$

b) Vertical ring load (Fig. 5b):

$$u_\rho = - R \sum_{\ell=1}^{2N} \phi_x^{m\ell} \phi_z^{n\ell} \frac{d}{d\rho} I_{4\ell}^{R} / k_\ell \tag{85a}$$

$$u_\theta = 0 \tag{85b}$$

$$u_z = R \sum_{\ell=1}^{2N} \phi_z^{m\ell} \phi_z^{n\ell} I_{4\ell}^{R} \tag{85c}$$

c) Torsional ring load (Fig. 5c):

$$u_\rho = 0 \tag{86a}$$

$$u_\theta = \sum_{\ell=1}^{N} \phi_y^{m\ell} \phi_y^{n\ell} (R\, I_{2\ell}^{L} - \frac{2}{R} I_{3\ell}^{L} + I_{1\ell}^{*L}) \tag{86b}$$

$$u_z = 0 \tag{86c}$$

d) Rocking (moment) ring load (Fig. 5d):

$$u_\rho = [\sum_{\ell=1}^{2N} \phi_x^{m\ell}\, \phi_z^{n\ell}\, \frac{d}{d\rho}\, (\frac{2}{R}\, I_{3\ell}^R - I_{1\ell}^{*R} - R\, I_{2\ell}^R)/k_\ell] \quad (\cos\theta) \tag{87a}$$

$$u_\theta = [\sum_{\ell=1}^{2N} \phi_x^{m\ell}\, \phi_z^{n\ell}\, \frac{1}{\rho}\, (\frac{2}{R}\, I_{3\ell}^R - I_{1\ell}^{*R} - R\, I_{2\ell}^R)/k_\ell] \quad (-\sin\theta) \tag{87b}$$

$$u_z = [\sum_{\ell=1}^{2N} \phi_z^{m\ell}\, \phi_z^{n\ell}\, (R\, I_{2\ell}^R - \frac{2}{R}\, I_{3\ell}^R + I_{1\ell}^R)\,] \quad (\cos\theta) \tag{87c}$$

2.6.4 Green functions for point loads

The Green functions for point loads can be obtained from those for disk loads by considering the limit when R tends to zero.

In the case of loads with intensity p, the corresponding tractions are

$$q = \frac{p}{\pi R^2} \qquad \text{(horizontal, vertical)}$$

The limiting expressions for the displacements when $R \to 0$ are given below.

a) Horizontal point load:

$$u_\rho = \frac{p}{4i} [\sum_{\ell=1}^{2N} \phi_x^{m\ell}\, \phi_x^{n\ell}\, \frac{d}{d\rho}\, H_1^{(2)}\, (k_\ell^R\rho)/k_\ell^R + \frac{1}{\rho} \sum_{\ell=1}^{N} \phi_y^{m\ell}\, \phi_y^{n\ell}\, H_1^{(2)}(k_\ell^2\rho)/k_\ell^L] \cos\theta$$

$$u_\theta = \frac{P}{4i} [\frac{1}{\rho} \sum_{\ell=1}^{2N} \phi_x^{m\ell}\, \phi_x^{n\ell}\, H_1^{(2)}\, (k_\ell^R\rho)/k_\ell^R + \sum_{\ell=1}^{N} \phi_y^{m\ell}\, \phi_y^{n\ell}\, H_1^{(2)}(k_\ell^L\rho)/k_\ell^L\,](-\sin\theta)$$

$$u_z = -\frac{p}{4i} \sum_{\ell=1}^{2N} \phi_z^{m\ell}\, \phi_x^{n\ell}\, H_1^{(2)}\, (k_\ell^R\rho)\,] \quad (\cos\theta) \tag{88a,b,c}$$

in which $H_j^{(2)}(k\rho)$ are second Hankel functions of j^{th} order.

b) Vertical point load:

$$u_\rho = \frac{P}{4i} \sum_{\ell=1}^{2N} \phi_x^{m\ell} \phi_z^{n\ell} H_1^{(2)}(k_\ell^R \rho) \tag{89a}$$

$$u_\theta = 0. \tag{89b}$$

$$u_z = \frac{P}{4i} \sum_{\ell=1}^{2N} \phi_z^{m\ell} \phi_z^{n\ell} H_0^{(2)}(k_\ell^R \rho) \quad . \tag{89c}$$

2.7 Green Functions for Internal Stresses

In applications of the Green function formalism to boundary value problems, particularly when using the Boundary Integral Method, it may be necessary to have expressions for the internal stresses induced by the loadings considered at arbitrary points in the soil mass.

Since the Green functions presented in this work have been derived using a discrete formulation, the internal stresses balance the external loads only in a finite element sense. Within the layers, there are body forces resulting from the linearization of the displacement field and from inertia forces that are balanced by consistent stresses applied at the layer interfaces. By comparison, in a finite element solution, there are body forces acting over the surface (volume) of the elements that are equilibrated by consistent nodal loads. The following sections present then expressions for these consistent loads and stresses.

2.7.1 Plane strain cases

a) Stresses due to antiplane line loads

We begin with the antiplane case, since it is the simplest, for it involves only one displacement component. In this case, two stress components are of interest, i.e., the shearing stresses γ_{xy}, γ_{yz} in vertical and horizontal planes.

Vertical planes:

With reference to Fig. 6 , the strain γ_{xy} in a vertical plane with abscissa x is

$$\gamma_{xy} = \frac{\partial u_y}{\partial x} \tag{90}$$

and in particular, the shearing strains at the elevation of the interfaces, arranged as a matrix, are

$$\Gamma_{xy} = \{\gamma_{xy}\}_{\text{interfaces}} = \frac{\partial}{\partial x}\left[\frac{1}{2i}\ \Phi_y\ E^L_{|x|} K_L^{-1}\ \Phi_y^T\right]$$

$$= \frac{1}{2i}\ \Phi_y\ \frac{\partial}{\partial x} E^L_{|x|} K_L^{-1}\ \Phi_y^T \tag{91}$$

which is obtained from the Green matrix for antiplane line loads, eq. (48).

But

$$\frac{\partial E_{|x|}}{\partial x} = -\ i\ E^L_{|x|}\ K_L \qquad \text{if } x > 0$$

$$= \quad i\ E^L_{|x|}\ K_L \qquad \text{if } x < 0 \tag{92}$$

Hence

$$\Gamma_{xy} = \mp\ \frac{1}{2}\ \Phi_y\ E^L_{|x|} \Phi_y^T \tag{93}$$

with the negative sign being associated with positive values of x and viceversa. We notice that the strains (and stresses) are discontinuous at x = 0. If the soil to the right of the section x considered is removed, it becomes then necessary to apply consistent antiplane line loads to the section to the left in order to preserve equilibrium with the internal stresses. The consistent nodal loads applied at the nodes defined by the intersection of the interfaces and the vertical plane considered can be obtained as follows:

Let $\gamma = \gamma_{xy}$ be the strain within the m^{th} layers, and γ_m, γ_{m+1} be the strains at the top and bottom of this layer. The shear modulus and thickness of the layer are G_m and h_m respectively. Since the strains γ_{xy} vary linearly within the layer (u_y and $\partial u_y/\partial z$ vary linearly with z), then

$$\gamma = \xi\gamma_m + (1-\xi)\gamma_{m+1}, \quad 0 \le \xi \le 1$$

$$= (\xi \quad 1-\xi) \begin{Bmatrix} \gamma_m \\ \gamma_{m+1} \end{Bmatrix} \tag{94}$$

The consistent nodal loads in equilibrium with the stresses $\tau = G_m\gamma$ are then

$$\begin{Bmatrix} Q_m \\ Q_{m+1} \end{Bmatrix} = G_m h_m \int_0^1 \begin{pmatrix} \xi \\ 1-\xi \end{pmatrix} (\xi \quad 1-\xi) \begin{Bmatrix} \gamma_m \\ \gamma_{m+1} \end{Bmatrix} d\xi$$

$$= \frac{G_m h_m}{6} \begin{bmatrix} 2 & 1 \\ 1 & 2 \end{bmatrix} \begin{Bmatrix} \gamma_m \\ \gamma_{m+1} \end{Bmatrix} = A_m \begin{Bmatrix} \gamma_m \\ \gamma_{m+1} \end{Bmatrix} \tag{95}$$

which constitutes the contribution of the m^{th} layer to the consistent nodal loads. Notice that A_m is the submatrix of the matrix A_m shown in table 1 that corresponds to the antiplane degrees of freedom. If all layers to the right of section x are removed, then the consistent nodal loads are obtained overlapping the contributions of all layers. This implies overlapping A_m (i.e., $A_y = \{A_m\}$). The result is

$$Q_y = A_y\Gamma = \mp \frac{1}{2} A_y \Phi_y E^L_{|x|} \Phi_y^T$$

$$= \mp i A_y \Phi_y K_L \Phi_y^{-1} \left| \frac{1}{2i} \Phi_y K_L^{-1} E^L_{|x|} \Phi_y^T \right|$$

$$= \mp i A_y \Phi_y K_L \Phi_y^{-1} U_y = \mp R U_y \tag{96}$$

since $K_L^{-1} E^L_{|x|} = E^L_{|x|} K_L^{-1}$. The matrix $R = i A_y \Phi_y K_L \Phi_y^{-1}$ is the Waas-Lysmer antiplane transmitting boundary (the dynamic stiffness matrix of the soil removed).

Observe that at x=0, $E^L_{|x|} = I$ (the identity matrix). Considering also the orthonormality condition $\Phi_y^T A_y \Phi_y = I$, we would have

$$Q_y = -\frac{1}{2} A_y \Phi_y \Phi_y^T = -\frac{1}{2} I \qquad \text{if} \quad x = 0^+ \tag{97a}$$

$$Q_y = \frac{1}{2} A_y \Phi_y \Phi_y^T = \frac{1}{2} I \qquad \text{if} \quad x = 0^- \tag{97b}$$

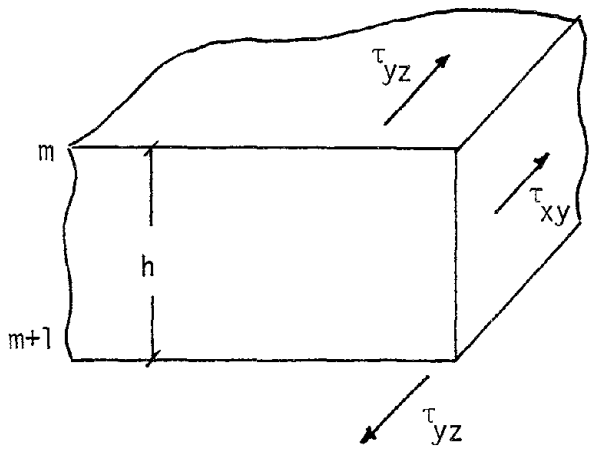

Stresses, antiplane case

Fig. 6

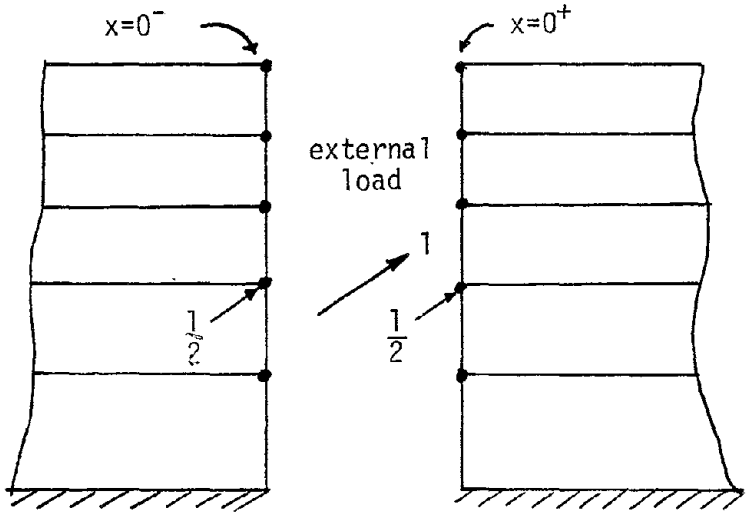

Internal consistent loads at x = 0

Fig. 7

Thus, the stresses are discontinuous, and the difference $\frac{1}{2}\,I - (-\frac{1}{2}\,I) = I$ balances the external loads applied (Fig. 7).

Horizontal planes

With reference to Fig. 6 and equation (9), the stresses $\bar{\tau} = \bar{\tau}_{yz}$ (in the wavenumber domain!) induced by antiplane displacements $\bar{v} = \bar{u}_y$ are

$$\begin{Bmatrix} \bar{\tau}_m \\ -\bar{\tau}_{m+1} \end{Bmatrix} = K_m \begin{Bmatrix} \bar{v}_m \\ \bar{v}_{m+1} \end{Bmatrix} \tag{98}$$

with K_m given by equation (11), considering only the antiplane degrees of freedom (i.e., K_m is a $\bar{4} \times \bar{4}$ matrix). From equation (38), the displacements at the interfaces m, m+1 due to a load at n can be written as ($k_\ell \equiv k_\ell^L$)

$$\begin{Bmatrix} v_m \\ v_{m+1} \end{Bmatrix} = \sum_{\ell=1}^{N} \frac{1}{k^2 - k_\ell^2} \begin{Bmatrix} \phi_y^{m\ell} \\ \phi_y^{m+1,\ell} \end{Bmatrix} \phi_y^{n\ell} \tag{99}$$

Hence

$$\begin{aligned} \begin{Bmatrix} \bar{\tau}_m \\ -\bar{\tau}_{m+1} \end{Bmatrix} &= \sum_{\ell=1}^{N} \frac{1}{k^2 - k_\ell^2} (A_m k^2 + G_m - \omega^2 M_m) \begin{Bmatrix} \phi_y^{m\ell} \\ \phi_y^{m+1,\ell} \end{Bmatrix} \phi_y^{n\ell} \\ &= \sum_{\ell=1}^{N} \left\{ \frac{1}{k^2 - k_\ell^2} (A_m k_\ell^2 + G_m - \omega^2 M_m) + A_m \right\} \begin{Bmatrix} \phi_y^{m\ell} \\ \phi_y^{m+1,\ell} \end{Bmatrix} \phi_y^{n\ell} \\ &= \sum_{\ell=1}^{N} \left\{ \frac{1}{k^2 - k_\ell^2} K_{m\ell} + A_m \right\} \begin{Bmatrix} \phi_y^{m\ell} \\ \phi_y^{m+1,\ell} \end{Bmatrix} \phi_y^{n\ell} \end{aligned} \tag{100}$$

in which

$$K_{m\ell} = K_m(k_\ell^L). \tag{101}$$

Taking an inverse Fourier transformation, we obtain then

$$\begin{Bmatrix} \tau_m \\ -\tau_{m+1} \end{Bmatrix} = \sum_{\ell=1}^{N} K_{m\ell} \begin{Bmatrix} \phi_y^{m\ell} \\ \phi_y^{m+1,\ell} \end{Bmatrix} \left(\frac{1}{2i} \frac{1}{k_\ell^L} \phi_y^{n\ell}\right) e^{-ik_\ell^L |x|} +$$

$$+ \sum_{\ell=1}^{N} \delta(x) A_m \begin{Bmatrix} \phi_y^{m\ell} \\ \phi_y^{m+1,\ell} \end{Bmatrix} \phi_y^{n\ell}$$

$$= \sum_{\ell=1}^{N} K_{m\ell} \begin{Bmatrix} \phi_y^{m\ell} \\ \phi_y^{m+1,\ell} \end{Bmatrix} \alpha_{n\ell} e^{-ik_\ell^L |x|} + \delta(x) A_m \sum_{\ell=1}^{N} \begin{Bmatrix} \phi_y^{m\ell} \\ \phi_y^{m+1,\ell} \end{Bmatrix} \phi_y^{n\ell} \quad (102)$$

in which

$$\alpha_{n\ell} = \frac{1}{2ik_\ell^L} \phi_y^{n\ell} \quad (103)$$

is the participation factor of the ℓ^{th} mode for an antiplane line load applied at the n^{th} interface. These stresses are "continuous" at the interfaces in the sense that they may be computed either with the layer above, or the layer below the interface of interest. This can be verified by overlapping the stress components for all layers, using for this purpose equation (102). The first summation would then cancel, since each term in ℓ is of the form $K\phi_y = 0$, which is zero, because the modes satisfy the quadratic eigenvalue problem referred to earlier in this report. The second term would be $\delta(x)A_y\Phi_y\Phi_y^T = \delta(x)I$, since $\Phi_y^T A_y \Phi_y = I$. Thus, the only singularity occurs at the location of the line loads.

b) Stresses due to in-plane line loads

Although the developments are somewhat more complicated than for the antiplane case because of the increase in the number of stress components, the generalization is straightforward, so that only the essential details need be presented. (Compare also with previous section.)

Vertical plane (Fig. 8):

$$\sigma_x = (\lambda + 2G)\frac{\partial u_x}{\partial x} + \lambda \frac{\partial u_z}{\partial z} \tag{104a}$$

$$\tau_{xz} = G\left(\frac{\partial u_x}{\partial z} + \frac{\partial u_z}{\partial x}\right) \tag{104b}$$

or in matrix form

$$\begin{Bmatrix} \sigma_x \\ \tau_{xz} \end{Bmatrix} = \left\{ \begin{bmatrix} \lambda + 2G & \\ & G \end{bmatrix} \frac{\partial}{\partial x} + \begin{bmatrix} & \lambda \\ G & \end{bmatrix} \frac{\partial}{\partial z} \right\} \begin{Bmatrix} u_x \\ u_z \end{Bmatrix} \tag{105}$$

Since both u_x, u_z vary linearly across the m^{th} layer,

$$\begin{Bmatrix} u_x \\ \\ u_z \end{Bmatrix} = U = \xi U_m + (1 - \xi) U_{m+1} \qquad 0 \leq \xi \leq 1 \tag{106}$$

or

$$U = \begin{Bmatrix} \xi & & 1-\xi & \\ & \xi & & 1-\xi \end{Bmatrix} \begin{Bmatrix} U_m \\ \\ U_{m+1} \end{Bmatrix} \tag{107}$$

and

$$\frac{\partial}{\partial z} U = \frac{1}{h_m} \begin{Bmatrix} 1 & & -1 & \\ & 1 & & -1 \end{Bmatrix} \begin{Bmatrix} U_m \\ \\ U_{m+1} \end{Bmatrix} \tag{108}$$

The consistent nodal loads in equilibrium with these stresses are then

$$\begin{Bmatrix} Q_m \\ Q_{m+1} \end{Bmatrix} = h_m \int_0^1 \begin{Bmatrix} \xi & \\ & \xi \\ 1-\xi & \\ & 1-\xi \end{Bmatrix} \begin{Bmatrix} \sigma_x \\ \tau_{xz} \end{Bmatrix} d\xi \tag{109}$$

or using (105, 107, 108) with $\lambda = \lambda_m$, $G = G_m$ (moduli for m^{th} layer, and integrating eq. (109):

$$\begin{Bmatrix} Q_m \\ Q_{m+1} \end{Bmatrix} = \left(A_m \frac{\partial}{\partial x} + D_m\right) \begin{Bmatrix} U_m \\ \\ U_{m+1} \end{Bmatrix} \tag{110}$$

in which A_m is again given in Table 1, with the antiplane degrees of freedom deleted (i.e., considering only rows/columns 1, 3, 4, 6) and U_m are the actual displacements at the m^{th} interface. Also, the matrix D_m is

$$D_m = \frac{1}{2} \begin{Bmatrix} 0 & \lambda & 0 & -\lambda \\ G & 0 & -G & 0 \\ 0 & \lambda & 0 & -\lambda \\ G & 0 & -G & 0 \end{Bmatrix} \tag{111}$$

Now, from equation (47), and considering the comment concerning the implicit factor $i = \sqrt{-1}$ on page 21, the actual displacements U_m at a given interface m due to line loads applied at the n^{th} interface are

$$U_m = \begin{Bmatrix} u_m \\ w_m \end{Bmatrix} = \sum_{\ell=1}^{2N} \left[\alpha_{n\ell} \begin{Bmatrix} \phi_x^{m\ell} \\ \mp i\phi_z^{m\ell} \end{Bmatrix} + i\beta_{n\ell} \begin{Bmatrix} \pm \phi_x^{m\ell} \\ -i\phi_z^{m\ell} \end{Bmatrix} \right] e^{-k_\ell^R |x|} \tag{112}$$

in which the choice of signs depends on whether $x > 0$ or $x < 0$. Also, the participation factor $\alpha_{n\ell}$ (for horizontal loads) and $\beta_{n\ell}$ (for vertical loads) are given by

$$\alpha_{n\ell} = \frac{1}{2i} \phi_x^{n\ell} / k_\ell^R \tag{113a}$$

$$\beta_{n\ell} = \frac{1}{2i} \phi_z^{n\ell} / k_\ell^R \tag{113b}$$

Equations (112) and (113) may be substituted into eq. (110) to evaluate the contribution of the m^{th} layer to the consistent internal loads. Considering now the special case in which all layers to the right of section x have been removed, we can write the consistent nodal load vector for the complete section as

$$\begin{Bmatrix} Q_x \\ Q_z \end{Bmatrix} = \frac{\partial}{\partial x} \begin{Bmatrix} A_z & \\ & A_z \end{Bmatrix} \begin{Bmatrix} U_x \\ U_z \end{Bmatrix} + \begin{Bmatrix} & D_{xz} \\ D_{zx} & \end{Bmatrix} \begin{Bmatrix} U_x \\ U_z \end{Bmatrix} \tag{114}$$

in which A_x, A_z have the same meaning as in section 2.4. It should be noted that Q_z, U_z in the above expression are the actual vertical loads and displacements, i.e., the i-factor has been removed. Also, D_{xz} and D_{zx} corresponds to an overlapping of the D_m - matrices (eq. (111)) for each layer, and a rearrangement of columns/rows by degrees of freedom rather than by interface. (Note that $D_{zx} \neq D_{xz}^T$). On the other hand, equation (47) transforms, after removal of the implicit factor $i = \sqrt{-1}$ referred to above, into

$$\begin{Bmatrix} u_x \\ u_z \end{Bmatrix} = \frac{1}{2i} \begin{Bmatrix} \Phi_x \\ \mp i\Phi_z \end{Bmatrix} E^R_{|x|} K_R^{-1} \left\{ \Phi_x^T \quad \pm i\Phi_z^T \right\} \tag{115}$$

or briefly,

$$U = \frac{1}{2i} \Phi E^R_{|x|} K_R^{-1} \tilde{\Phi}^T \qquad x > 0 \tag{116a}$$

$$U = \frac{1}{2i} \tilde{\Phi} E^R_{|x|} K_R^{-1} \Phi^T \qquad x < 0 \tag{116b}$$

in which

$$\Phi = \begin{Bmatrix} \Phi_x \\ -i\Phi_z \end{Bmatrix} \quad , \quad \tilde{\Phi} = \begin{Bmatrix} \Phi_x \\ i\Phi_z \end{Bmatrix} \tag{117}$$

Combining (114) and (116), one obtains for $x > 0$

$$\begin{aligned} Q &= \frac{1}{2i} \left\{ -i A \Phi E^R_{|x|} \tilde{\Phi}^T + D \Phi E^R_{|x|} K_R^{-1} \tilde{\Phi}^T \right\} \\ &= -\frac{1}{2i} \left\{ i A \Phi K_R \Phi^{-1} - D \right\} \Phi K_R^{-1} E^R_{|x|} \tilde{\Phi}^T \\ &= -R U \qquad , \qquad R = i A \Phi K_R \Phi^{-1} - D \end{aligned} \tag{118}$$

and for $x < 0$,

$$\begin{aligned} Q &= \frac{1}{2i} \left\{ i A \tilde{\Phi} K_R \tilde{\Phi}^{-1} + D \right\} \tilde{\Phi} K_R^{-1} E^R_{|x|} \Phi^T \\ &= L U \qquad , \qquad L = i A \tilde{\Phi} K_R \tilde{\Phi}^{-1} + D \end{aligned} \tag{119}$$

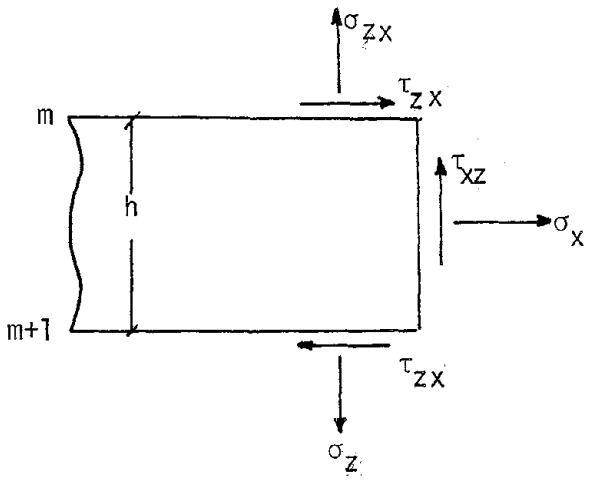

Stresses, in plane case

Fig. 8

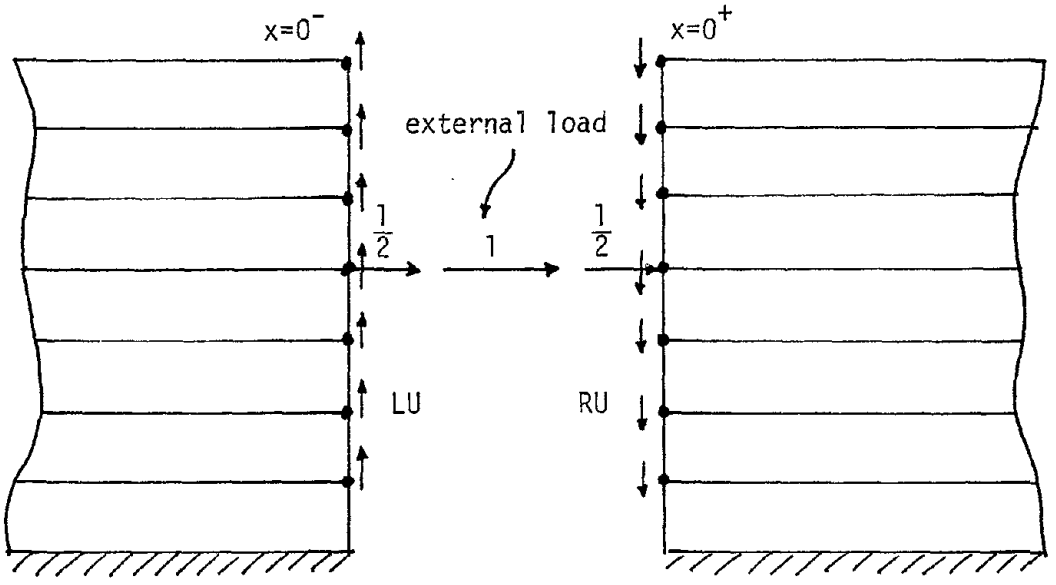

Internal consistent loads at x=0
(horizontal load)

Fig. 9

In equations (118, 119) the expressions for R, L give the stiffness matrices for the Waas-Lysmer transmitting boundaries corresponding to the right and left layered regions that stretch from $x > 0$ to ∞, or from $x < 0$ to $-\infty$, respectively. The matrix L follows trivially from the matrix R by changing the sign of the terms coupling the horizontal and vertical degrees of freedom. (See also Waas, 1972).

Horizontal planes (Fig. 8)

The stresses are obtained again by a Fourier transformation of the stress components in the wavenumber domain, which in turn are given by the product of the layer stiffness matrix times the layer displacements that follow from equation (37). The only difference with the antiplane case is the presence of the factor k in the coupling terms, that may be changed into a factor 1/k via equation (32). The result of the Fourier transformation is (compare with eq. (102))

$$\begin{Bmatrix} \tau_m \\ i\sigma_m \\ -\tau_{m+1} \\ -i\sigma_{m+1} \end{Bmatrix} = \sum_{\ell=1}^{2N} K_{m\ell} \begin{Bmatrix} \phi_x^{m\ell} \\ \phi_z^{m\ell} \\ \phi_x^{m+1,\ell} \\ \phi_z^{m+1,\ell} \end{Bmatrix} \begin{pmatrix} \alpha_{n\ell} \\ \beta_{n\ell} \end{pmatrix} e^{-ik_\ell^R x} + S_n \qquad x \geq 0 \tag{120}$$

with $K_{m\ell} = K_m(k_\ell^R)$ given by equation (11), with antiplane degrees of freedom deleted. Also, the choice of participation factors $\alpha_{n\ell}$ or $\beta_{n\ell}$, which are given by eqution (113), depends on whether a horizontal or vertical load is considered. The additional singularity term S_n is given by

$$S_n = \delta(x)\, A_m \sum_{\ell=1}^{2N} \begin{Bmatrix} 0 \\ \phi_x^{m,\ell} \\ 0 \\ \phi_x^{m+1,\ell} \\ 0 \end{Bmatrix} \phi_x^{n\ell} \tag{121a}$$

for horizontal loads, and

$$S_n = \delta(x)\, A_m \sum_{\ell=1}^{2N} \begin{Bmatrix} 0 \\ \phi_z^{m,\ell} \\ 0 \\ \phi_z^{m+1,\ell} \end{Bmatrix} \phi_z^{n\ell} \tag{121b}$$

for vertical loads.

To obtain the stresses for $x < 0$, one simply reverses the sign of σ for horizontal loads, or the sign of τ for vertical loads.

Again, these stresses are "continuous" at the interfaces, since overlapping cancels the first summation in eq. (120); (satisfies eigenvalue problem). The singularity terms become

$$\left.\begin{aligned} T &= \delta(x)\, A_x\, \Phi_x\, \Phi_x^T = \delta(x)\, I \\ iS &= 0 \end{aligned}\right\} \quad \text{for horizontal loads} \tag{122a}$$

$$\left.\begin{aligned} T &= 0 \\ iS &= \delta(x)\, A_z\, \Phi_z\, \Phi_z^T = \delta(x)\, I \end{aligned}\right\} \quad \text{for vertical loads} \tag{122b}$$

The above relationships can be proven via the orthogonality condition specified by Eq. (22a): (Also see Appendix)

$$(K_R\, \Phi_x^T\, \Phi_z^T) \begin{Bmatrix} A_x & \\ B_{xz} & A_z \end{Bmatrix} \begin{Bmatrix} \Phi_x & \\ & \Phi_z \end{Bmatrix} = K_R \tag{123}$$

or
$$K_R\, \Phi_x^T\, A_x\, \Phi_x + \Phi_z^T\, A_z\, \Phi_z\, K_R + \Phi_z^T\, B_{xz}\, \Phi_x = K_R \tag{124}$$

Multiplying from the left by $\Phi_x\, K_R^{-1}$, we obtain

$$\Phi_x\, \Phi_x^T\, A_x\, \Phi_x + (\Phi_x\, K_R^{-1}\, \Phi_z^T)(A_z\, \Phi_z\, K_R + B_{xz}\, \Phi_x) = \Phi_x \tag{125}$$

But in view of equation (34), the second term cancels. Hence

$$\Phi_x\, \Phi_x^T\, A_x \Phi_x = \Phi_x \tag{126}$$

implying that $\Phi_x\, \Phi_x^T\, A_x = I$, or

$$A_x\, \Phi_x\, \Phi_x^T = I \tag{127}$$

Also, the relationship

$$A_z\, \Phi_z\, \Phi_z^T = I \tag{128}$$

can be proven by multiplying eq. (124) by $K_R^{-1}\ \Phi_z^T$ from the right, and proceding as above. It follows that the only singularities occur under the line loads (Fig. 9).

2.7.2 Cylindrical case

While the formulation of the stresses in cylindrical coordinates generally parallels that of the two plane-strain cases, the resulting expressions are more involved, both formally as well as computationally. However, since the concept remains the same, only a sketch of the developments is necessary.

Vertical (cylindrical) plane (Fig. 10)

$$\begin{Bmatrix} \sigma_\rho \\ \tau_{\rho\theta} \\ \tau_{\rho z} \end{Bmatrix} = \left\{ \begin{bmatrix} \lambda+2G & . & . \\ . & G & . \\ . & . & . \end{bmatrix} \frac{\partial}{\partial \rho} + \begin{bmatrix} . & . & \lambda \\ . & . & . \\ G & . & . \end{bmatrix} \frac{\partial}{\partial z} + \begin{bmatrix} \lambda & -\mu\lambda & . \\ \mu G & -G & . \\ . & . & . \end{bmatrix} \frac{1}{\rho} \right\} \begin{Bmatrix} u_\rho \\ u_\theta \\ u_z \end{Bmatrix} \tag{129}$$

Both the stress and displacement vectors must be multiplied by T_μ (eqs. (6 a, 6b)) in order to incorporate the variation with the azimuth.

Considering again a linear variation of the displacements across a layer, that is,

$$U = \xi U_m + (1 - \xi) U_{m+1} \qquad 0 \leq \xi \leq 1 \tag{130}$$

one obtains for the consistent nodal loads

$$\begin{Bmatrix} Q_m \\ Q_{m+1} \end{Bmatrix} = \left(A_m \frac{\partial}{\partial \rho} + D_m + \frac{1}{\rho} E_m \right) \begin{Bmatrix} U_m \\ U_{m+1} \end{Bmatrix} \tag{131}$$

in which A_m is again given in table 1 and D_m, E_m are the matrices

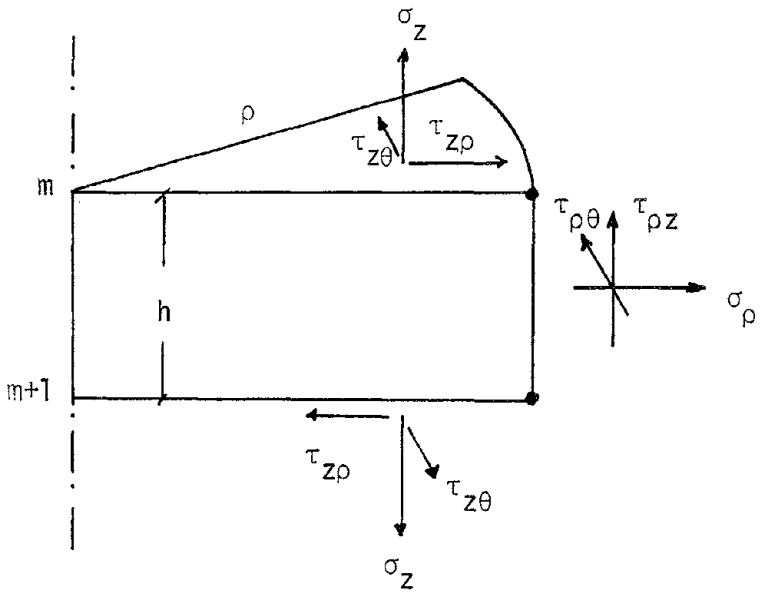

Stresses, Cylindrical coordinates

Fig. 10

$$D_m = \frac{1}{2} \begin{Bmatrix} . & . & \lambda & . & . & -\lambda \\ . & . & . & . & . & . \\ G & . & . & -G & . & . \\ . & . & \lambda & . & . & -\lambda \\ . & . & . & . & . & . \\ G & . & . & -G & . & . \end{Bmatrix} \tag{132}$$

$$E_m = \frac{h}{6} \begin{Bmatrix} 2\lambda & -2\mu\lambda & . & \lambda & -\mu\lambda & . \\ 2\mu G & -2G & . & G & -G & . \\ . & . & . & . & . & . \\ \lambda & -\mu\lambda & . & 2\lambda & -2\mu\lambda & . \\ \mu G & -G & . & 2\mu G & -2G & . \\ . & . & . & . & . & . \end{Bmatrix} \tag{133}$$

Note that eq. (132) differs from eq. (111) only in that two rows/columns of zeroes have been added.

Equation (131) may then be used to compute the stresses with U_m (and U_{m+1}) given by the equations for the Green functions presented in section 2.6, but omitting the factors $\cos \mu\theta$, $-\sin \mu\theta$ etc.

Again, in the particular case in which all the soil beyond the section ρ has been removed, the consistent nodal load vector will be given by an expression of the form (compare with eq. (131)

$$Q = (A \frac{\partial}{\partial \rho} + D + \frac{1}{\rho} E)\, U \tag{134}$$

with A, D, E being the overlapped matrices for the whole soil profile. Hence, if U is a Green matrix,

$$Q = (A\, U'\, U^{-1} + D + \frac{1}{\rho} E)\, U \tag{135}$$

with
$$U' = \frac{\partial}{\partial \rho} U \tag{136}$$

which relates consistent nodal loads (per unit circle length) to displacements. It follows that

$$R = -\rho(A\,U'U^{-1} + D + \frac{1}{\rho}E) \tag{137}$$

is the stiffness matrix of the transmitting boundary with radius ρ relating nodal loads/radian applied on the boundary (having the variation with azimuth implied by T_μ) with corresponding displacements there. While in principle any (linearly independent) combination of solutions having common Fourier index μ could be used to form the Green matrix ($\rho > R$!), it is best to use the solutions for point loads and moments. These ideas will not, however, be pursued here.

Horizontal planes

While in the plane strain cases the stresses are obtained by Fourier-transformation of the corresponding expressions in the wave-number domain, in the cylindrical case they follow from Hankel transformations, which are inherently more involved. Nevertheless, the integrations can still be concarried out in closed form.

With reference to equations (4) through (11), the stresses at elevation m, m+1 are

$$\begin{Bmatrix} S_m \\ -S_{m+1} \end{Bmatrix} = \sum_{\mu=0}^{\infty} \begin{Bmatrix} T_\mu & \\ & T_\mu \end{Bmatrix} \int_0^\infty k \begin{Bmatrix} C_\mu & \\ & C_\mu \end{Bmatrix} K_m \begin{Bmatrix} \overline{U}_m \\ \overline{U}_{m+1} \end{Bmatrix} dk \tag{138}$$

in which $\overline{U}_m$, $\overline{U}_{m+1}$ are the displacement vectors in the wave-number domain at these elevations. The actual displacements (e.g., 5a repeated) are

$$U_m = \sum_{\mu=0}^{\infty} T_\mu \int_o^\infty k\, C_\mu\, \overline{U}_m\, dk \tag{139}$$

and a similar expression for U_{m+1}.

On the other hand, with reference to equations (51), (52) and (53), $\overline{U}_m$ (and $\overline{U}_{m+1}$) can be written as: (The equivalent forms are due to equations (51b,c)

$$\bar{U}_m = f(k,R) \sum_{\ell=1}^{3N} a_\ell \begin{Bmatrix} \phi_x^{m\ell} \\ \phi_y^{m\ell} \\ \frac{k_\ell}{k} \phi_z^{m\ell} \end{Bmatrix} \alpha_{n\ell} = f(k,R) \sum_{\ell=1}^{3N} a_\ell \begin{Bmatrix} \phi_x^{m\ell} \\ \phi_y^{m\ell} \\ \frac{k}{k_\ell} \phi_z^{m\ell} \end{Bmatrix} \alpha_{n\ell} \tag{140}$$

for radial-tangential loads, and

$$\bar{U}_m = f(k,R) \sum_{\ell=1}^{3N} a_\ell \begin{Bmatrix} \frac{k_\ell}{k} \phi_x^{m\ell} \\ \phi_y^{m\ell} \\ \phi_z^{m\ell} \end{Bmatrix} \alpha_{n\ell} = f(k,R) \sum_{\ell=1}^{3N} a_\ell \begin{Bmatrix} \frac{k}{k_\ell} \phi_x^{m\ell} \\ \phi_y^{m\ell} \\ \phi_z^{m\ell} \end{Bmatrix} \alpha_{n\ell} \tag{141}$$

for vertical-torsional loads.

In these equations, $f(k,R)$ accounts for the variation of the load with the wavenumber k, and $\alpha_{n\ell}$ is the "participation factor" of the ℓ^{th} mode for a load applied at the n^{th} interface. The modes $\phi_x^{m\ell}$, $\phi_y^{m\ell}$, $\phi_z^{m\ell}$ used above correspond to a generalization of equation (50) in the following sense:

$$\left.\begin{array}{lll} \text{a) for} & 1 \le \ell \le 2N & \text{("Rayleigh modes")} \\ & \phi_y^{m\ell} = 0 & \\ & k_\ell = k_\ell^R & \\ \text{b) for} & 2N+1 \le \ell \le 3N & \text{("Love modes")} \\ & \phi_x^{m\ell} = \phi_z^{m\ell} = 0 & \\ & k_\ell = k_\ell^L & \end{array}\right\} \tag{142}$$

All that has been done then in (140), (141) is to combine Rayleigh and Love modes into a single summation, shifting the index of the latter by 2N. These equations can also be expressed more compactly as

$$\bar{U}_m = f(k,R) \sum_{\ell=1}^{3N} a_\ell \, Q_\ell \, \Phi_{m\ell} \, \alpha_{n\ell} \tag{143a}$$

$$= f(k,R) \sum_{\ell=1}^{3N} a_\ell \, Q_\ell^{-1} \, \Phi_{m\ell} \, \alpha_{n\ell} \tag{143b}$$

in which

$$Q_\ell = \begin{Bmatrix} 1 & & \\ & 1 & \\ & & \frac{k_\ell}{k} \end{Bmatrix} \tag{144}$$

corresponds to equation (140), and

$$Q_\ell = \begin{Bmatrix} \frac{k_\ell}{k} & & \\ & 1 & \\ & & 1 \end{Bmatrix} \tag{145}$$

is used for equation (141). Also

$$\Phi_{m\ell} = \begin{Bmatrix} \phi_x^{m\ell} \\ \phi_y^{m\ell} \\ \phi_z^{m\ell} \end{Bmatrix} \tag{146}$$

Substituting equation (143a) into (139), interchanging summation over ℓ with integration over k, we obtain

$$U_m = \sum_{\mu=0}^{\infty} T_\mu \sum_{\ell=1}^{3N} \alpha_{n\ell} \left\{ \int_0^{\infty} k\, C_\mu\, Q_\ell\, a_\ell\, f(k,R)dk \right\} \Phi_{m\ell}$$

$$= \sum_{\mu=0}^{\infty} T_\mu \sum_{\ell=1}^{3N} \alpha_{n\ell}\, H_\ell\, \Phi_{m\ell} \tag{147}$$

in which

$$H_\ell = \int_0^{\infty} k\, C_\mu\, Q_\ell\, a_\ell\, f(k,R)\, dk \tag{148}$$

For example, equations (60), giving the Green functions for a horizontal disk load can be written in the compact form (147), with μ=1 being the only non-zero term in the summation over the Fourier index, and

$$H_\ell = \begin{Bmatrix} \frac{d}{d\rho} I_{3\ell} & \frac{1}{\rho} I_{3\ell} & \\ \frac{1}{\rho} I_{3\ell} & \frac{d}{d\rho} I_{3\ell} & \\ & & -k_\ell I_{3\ell} \end{Bmatrix}$$

$$\alpha_{n\ell} = \begin{cases} qR\ \phi_x^{n\ell}, & 1 \le \ell \le 2N \\ qR\ \phi_y^{n\ell}, & 2N+1 \le \ell \le 3N \end{cases}$$

Alternatively, when substituting equation (143b) into (139), we obtain

$$U_m = \sum_{\mu=0}^{\infty} T_\mu \sum_{\ell=1}^{3N} \alpha_{n\ell} \left\{ \int_0^\infty k\, C_\mu\, Q_\ell^{-1}\, a_\ell\, f(k,R)dk \right\} \Phi_{m\ell}$$

$$= \sum_{\mu=0}^{\infty} T_\mu \sum_{\ell=1}^{3N} \alpha_{n\ell}\, \bar{H}_\ell\, \Phi_{m\ell} \qquad (149)$$

in which

$$\bar{H}_\ell = \int_0^\infty k\, C_\mu\, Q_\ell^{-1}\, a_\ell\, f(k,R)dk \qquad (150)$$

Note that while $H_\ell \neq \bar{H}_\ell$, the net summation is the same.

Returning now to the problem of determining the stresses in horizontal planes, let us consider once more equation (11):

$$K_m = A_m k^2 + B_m k + G_m - \omega^2 M_m \qquad (151)$$

Because of the special structure of the matrices involved (table 1), the following can be established:

$$A_m \begin{Bmatrix} Q_\ell & \\ & Q_\ell \end{Bmatrix} = \begin{Bmatrix} Q_\ell & \\ & Q_\ell \end{Bmatrix} A_m \tag{152a}$$

$$B_m \begin{Bmatrix} Q_\ell^{-1} & \\ & Q_\ell^{-1} \end{Bmatrix} = \frac{k}{k_\ell} \begin{Bmatrix} Q_\ell & \\ & Q_\ell \end{Bmatrix} B_m \tag{152b}$$

$$(G_m - \omega^2 M_m) \begin{Bmatrix} Q_\ell & \\ & Q_\ell \end{Bmatrix} = \begin{Bmatrix} Q_\ell & \\ & Q_\ell \end{Bmatrix} (G_m - \omega^2 M_m) \tag{152c}$$

Hence

$$\begin{aligned} a_\ell K_m \begin{Bmatrix} Q_\ell & \\ & Q_\ell \end{Bmatrix} &=: a \begin{Bmatrix} Q_\ell & \\ & Q_\ell \end{Bmatrix} \left\{ k^2 A_m + \frac{k^2}{k_\ell} B_m + G_m - \omega^2 M_m \right\} \\ &=: a_\ell \begin{Bmatrix} Q_\ell & \\ & Q_\ell \end{Bmatrix} \left\{ k_\ell^2 A_m + k_\ell B_m + G_m - \omega^2 M_m \right\} + \\ &+ \begin{Bmatrix} Q_\ell & \\ & Q_\ell \end{Bmatrix} \left\{ A_m + \frac{1}{k_\ell} B_m \right\} \end{aligned} \tag{153}$$

The sign =: indicates not an equality, but an equivalence (because of (152b); however, it becomes an equality after summation over ℓ, for the same reason that (143a,b) are equal.

Substituting then equations (143a,b) into equation (138), and considering equations (148), (153), we obtain

$$\begin{aligned} \begin{Bmatrix} S_m \\ -S_{m+1} \end{Bmatrix} = \sum_{\mu=0}^{\infty} \begin{Bmatrix} T_\mu & \\ & T_\mu \end{Bmatrix} \sum_{\ell=0}^{3N} \alpha_{n\ell} \Bigg[\begin{Bmatrix} H_\ell & \\ & H_\ell \end{Bmatrix} K_{m\ell} \begin{Bmatrix} \Phi_{m\ell} \\ \Phi_{m+1,\ell} \end{Bmatrix} + \\ + \left\{ \int_0^\infty k \begin{Bmatrix} C_\mu Q_\ell & \\ & C_\mu Q_\ell \end{Bmatrix} f(k,R)dk \right\} \begin{Bmatrix} A_m + \frac{1}{k_\ell} B_m \end{Bmatrix} \begin{Bmatrix} \Phi_{m\ell} \\ \Phi_{m,\ell} \end{Bmatrix} \Bigg] \end{aligned} \tag{154}$$

in which $K_{m\ell} = K_m(k_\ell) = A_m k_\ell^2 + B_m k_\ell + G_m - \omega^2 M_m$. Defining the modal stresses

$$\begin{Bmatrix} S_{m\ell} \\ S_{m+1,\ell} \end{Bmatrix} = K_{m\ell} \begin{Bmatrix} \Phi_{m\ell} \\ \Phi_{m+1,\ell} \end{Bmatrix} \tag{155}$$

and the "truncated" modal stresses

$$\begin{aligned} \begin{Bmatrix} \tilde{S}_{m,\ell} \\ \tilde{S}_{m+1,\ell} \end{Bmatrix} &= (A_m k_\ell^2 + B_m k_\ell) \begin{Bmatrix} \Phi_{m\ell} \\ \Phi_{m+1,\ell} \end{Bmatrix} \\ &= \left\{ K_{m\ell} - (G_m - \omega^2 M_m) \right\} \begin{Bmatrix} \Phi_{m\ell} \\ \Phi_{m+1,\ell} \end{Bmatrix} \end{aligned} \tag{156}$$

The interface stresses are then

$$S_m = \sum_{\mu=0}^{\infty} T_\mu \sum_{\ell=1}^{3N} \alpha_{n\ell} (H_\ell S_{m\ell} + L_\ell \tilde{S}_{m\ell}) \tag{157}$$

with the shorthand

$$L_\ell = \frac{1}{k_\ell^2} \int_0^\infty k C_\mu Q_\ell f(k,R)dk \tag{158}$$

Example

Consider again the case of a horizontal disk load; we would have then

$$\mu = 1 \quad , \quad f(k,R) = J_1(kR)/k$$

$$L_\ell = \frac{1}{k_\ell^2} \int_0^\infty \left\{ \begin{array}{cc|c} \frac{d}{dk\rho} J_1 & \frac{1}{k\rho} J_1 & \\ \frac{1}{k\rho} J_1 & \frac{d}{dk\rho} J_1 & \\ \hline & & -\frac{k_\ell}{k} J_1 \end{array} \right\} J_1(kR)dk$$

with $J_1 = J_1(k_\ell \rho)$. Integration gives

$$L_\ell = \frac{1}{k_\ell^2}\ \frac{1}{2R}\begin{Bmatrix} 1 & 1 & & \\ 1 & 1 & & \\ & & & -k_\ell\rho \end{Bmatrix} \qquad 0 \le \rho \le R$$

$$= \frac{1}{k_\ell^2}\ \frac{R}{2\rho^2}\begin{Bmatrix} -1 & 1 & & \\ 1 & -1 & & \\ & & & -k_\ell\rho \end{Bmatrix} \qquad R \le \rho < \infty$$

It remains to show that when the above expressions are introduced into (154), (157) the correct expressions for the stresses are obtained. For this purpose, we overlap the stresses at each interface to obtain the external forces. From equation (154), the overlapped stress vector will contain terms of the form $K\Phi_\ell$, which will cancel because they satisfy the eigenvalue equation. The only terms that will survive are those in $\{L_\ell\ \tilde{S}_{m\ell}\}$; of these, we see from equation (154) that only the term $-(G - \omega^2 M)\Phi_\ell$ will contribute, since the one in $K\Phi_\ell$ cancels for the same reason as above. The load vector will then be given by

$$P = -\sum_{\ell=1}^{3N} \begin{Bmatrix} T_1 L_\ell & & & \\ & \ddots & & \\ & & & T_1 L_\ell \end{Bmatrix} (G - \omega^2 M)\Phi_\ell\ \alpha_{n\ell}$$

As before, we can rearrange the components by degree of freedom rather than by interface. This would give, after consideration of the structure of the matrices G, M, L:

$$P = -q\ f(\rho) \begin{Bmatrix} (\cos\theta)\ [\pm\ (G_x - \omega^2 M_x)\Phi_x K_R^{-2}\ \Phi_x^T + (G_y - \omega^2 M_y)\Phi_y\ K_L^{-2}\ \Phi_y^T] \\ (-\sin\theta)\ [\ (G_x - \omega^2 M_x)\Phi_x K_R^{-2}\ \Phi_x^T \pm (G_y - \omega^2 M_y)\Phi_y\ K_L^{-2}\ \Phi_y^T] \\ (\cos\theta)\ [-\rho(G_z - \omega^2 M_z)\Phi_z K_R^{-1}\Phi_x^T] \end{Bmatrix}$$

in which $f(\rho) = \frac{1}{2}$ $\qquad 0 \le \rho \le R$, $\qquad$ use (+) sign

$$= \frac{R}{2\rho^2} \qquad R \le \rho \le \infty\ , \qquad \text{use (-) sign}$$

(The factor K^{-2} comes from the term $1/k_\ell^2$ in front of L_ℓ, and Φ_x^T, Φ_y^T are from the participation factors).

But from equation (34), the third row cancels. Also, we shall prove that the first two rows are equal to -2I (twice the identity matrix) if $\rho \leq R$, and zero if $\ell > R$. (because of the sign change). Hence

$$P = q \begin{Bmatrix} (\cos\theta)\ I \\ (-\sin\theta)\ I \\ 0 \end{Bmatrix} \qquad 0 \leq \rho \leq R$$

which is the correct result (compare with equation (54).

To prove the relationships used above, consider once more the orthogonality condition expressed by equation (22b): (Also see Appendix)

$$(K_R\ \Phi_x^T \quad \Phi_z^T) \begin{bmatrix} C_x & B_{xz} \\ & C_z \end{bmatrix} \begin{Bmatrix} \Phi_x \\ \Phi_z K_R \end{Bmatrix} = -\ K_R^3 \tag{159}$$

in which $C_x = G_x - \omega^2 M_x$, $C_z = G_z - \omega^2 M_z$. Expanding this equation, we obtain:

$$K_R\ \Phi_x^T\ C_x\ \Phi_x + K_R\ \Phi_x^T\ B_{xz}\ \Phi_z\ K_R + \Phi_c^T\ C_z\ \Phi_z\ K_R = -\ K_R^3 \tag{160}$$

Multiplying by $K_R^{-2}\ \Phi_x^T$ from the right and by K_R^{-1} from the left, we obtain

$$\Phi_x^T\ C_x \Phi_x\ K_R^{-2} \Phi_x^T + \Phi_x^T\ B_{xz}\ \Phi_z\ K_R^{-1} \Phi_x^T + K_R^{-1} \Phi_z^T\ C_z\ \Phi_z\ K_R^{-1}\ \Phi_x^T = -\ \Phi_x^T \tag{161}$$

But from equation (34) the second and third terms cancel, Thus, (161) reduces to

$$\Phi_x^T\ C_x\ \Phi_x\ K_R^{-2} \Phi_x^T = -\ \Phi_x^T \tag{162}$$

Multiplying by Φ_x from the left, and then by $(\Phi_x\ \Phi_x^T)^{-1}$ (barring the case of a singular square matrix $\Phi_x\ \Phi_x^T$), we obtain

$$C_x\ \Phi_x\ K_R^{-2} \Phi_x^T = -\ I \tag{163}$$

and

$$\Phi_x\ K_R^{-2}\ \Phi_x^T = -\ C_x^{-1} \tag{164}$$

In a similar way, the expression

$$\Phi_z \, K_R^{-2} \, \Phi_z^T = - \, C_z^{-1} \tag{165}$$

can be demonstrated from equation (160) with a factor $\Phi_z \, K_R^{-2}$ from the left, a factor K_R^{-1} from the right, and proceding as before. Finally, from equation (22b) we can also find for the antiplane case

$$\Phi_y^T \, C_y \, \Phi_y = - \, K_L^2 \tag{166}$$

In this case, Φ_y is a square, non-singular matrix. Hence

$$C_y = - \, \Phi_y^{-T} \, K_L^2 \, \Phi_y^{-1} \tag{167}$$

and

$$\Phi_y \, K_L^{-2} \, \Phi_y^T = - \, C_y^{-1} \tag{168}$$

In order to apply equation (157) (or (154)) to the computation of the stresses, it is necessary to express the displacements (Green functions) as in equation (147). For the various cases considered before, the matrices H_ℓ, L_ℓ (eqs. (148), (158)) have the structure: (However, see note below.)

$$H_\ell = \begin{Bmatrix} \frac{d}{d\rho} f_\ell & \frac{\mu}{\rho} f_\ell & \\ \frac{\mu}{\rho} f_\ell & \frac{d}{d\rho} f_\ell & \\ & & -k_\ell \, f_\ell \end{Bmatrix} \tag{169}$$

$$L_\ell = \frac{1}{k_\ell^2} \begin{Bmatrix} \frac{d}{d\rho} g & \frac{\mu}{\rho} g & \\ \frac{\mu}{\rho} g & \frac{d}{d\rho} g & \\ & & -k_\ell g \end{Bmatrix} \tag{170}$$

in which $f_\ell = f_\ell(k_\ell \rho)$, $g = g(\rho, R)$ (Compare with equation (7)). These functions are listed in table 3, together with other relevant data .

(Note: The matrices H_ℓ, L_ℓ are not symmetric if Q_ℓ is defined by eq. (145) (vertical loads). However, in this case the participation factor of the antiplane modes ($\ell > 2N$) is zero; hence, no error arises from using a symmetric form , provided it is properly defined.)

Table 3

Case	Load	Fourier Index μ	$\alpha_{n\ell}$ $1 \le \ell \le 2N$	$\alpha_{n\ell}$ $2N+1 \le \ell \le 3N$	f_ℓ	g $0 \le \rho < R$	g $R \le \rho < \infty$
1	Horizontal Disk	1	$qR\phi_x^{n\ell}$	$qR\phi_y^{n\ell}$	$I_{3\ell}$	$\frac{\rho}{2R}$	$\frac{R}{2\rho}$
2	Vertical Disk	0	$qR\phi_z^{n\ell}$	0	$-I_{1\ell}/k_\ell$	$-\frac{1}{k_\ell R}$	0
3	Torsional Disk	0	0	$qR\phi_y^{n\ell}$	$\int(\frac{2}{R} I_{3\ell} - \bar{I}^*_{1\ell})d\rho$	$\frac{1}{2}(\frac{\rho}{R})^2$ + const	0
4	Rocking Disk	1	$qR\phi_z^{n\ell}$	0	$(I^*_{1\ell} - \frac{2}{R} I_{3\ell})/k_\ell$	$-\frac{\rho}{k_\ell R^2}$	0
5	Horizontal Ring	1	$R\phi_x^{n\ell}$	$R\phi_y^{n\ell}$	$I^*_{1\ell}$		
6	Vertical Ring	0	$R\phi_z^{n\ell}$	0	$-I_{4\ell}/k_\ell$		
7	Torsional Ring	0	0	$R\phi_y^{n\ell}$	$\int(I_{2\ell} + \frac{1}{R} I_{1\ell} - \frac{2}{R^2} I_{3\ell})d\rho$		
8	Rocking Ring	1	$R\phi_z^{n\ell}$	0	$(\frac{2}{R^2} I_{3\ell} - \frac{1}{R} I_{1\ell} - I_{2\ell})/k_\ell$		
9	Horizontal Point	1	$P\phi_x^{n\ell}/4i$	$P\phi_y^{n\ell}/4i$	$H_1^{(2)}/k_\ell$		
10	Vertical Point	0	$P\phi_z^{n\ell}/4i$	0	$-H_0^{(2)}/k_\ell$		

3 - EXAMPLE: HORIZONTAL AND VERTICAL DISK LOADS

The discrete method described in the preceding section has been implemented in a computer program that may be used to evaluate the Green functions for an arbitrarily layered stratum. In order to verify the theory as well as the program, comparisons were performed for some particular cases with the results obtained with the "exact" solution (i.e., formulating the functions with the continuum theory in the wavenumber domain, and integrating numerically). This section presents the results of some of these comparisons.

Consider the case of a homogeneous stratum, subjected to a horizontal or vertical disk load at its free surface. The stratum is then discretized with N sublayers, following criteria similar to those applicable to finite elements. For the case at hand, the calculations were repeated for three discretization schemes: N = 4, N = 6, and N = 12 (Fig. 11), and covering in each case a range of frequencies.

Figure 12 presents the average horizontal displacement under the load as a function of 1/N. Fig. 13 depicts the corresponding data for a vertical load. These average displacements approximate closely the lateral or vertical compliance of a rigid disk having the same radius and location as the load. The three data points denoted by an (x) correspond to the results obtained with the discrete algorithm, while the point (0) on the vertical axis was obtained with the "exact" solution scheme. It may be observed that the error introduced as a result of discretizing the displacement field is small, particularly in the case of 12 layers. Notice also that the discretization increases the stiffness (and reduces the compliance) of the system, because of the constraints on the displacement field.

Figures 14 through 19 show the Green functions in terms of the dimensionless frequency $f_0 = fH/C_s$, in which f is the circular frequency (in Hz), H is the depth of the stratum, and C_s is the shear wave velocity). Again, there is a good agreement between the discrete and "exact" solutions, particularly for the imaginary part, as well as at

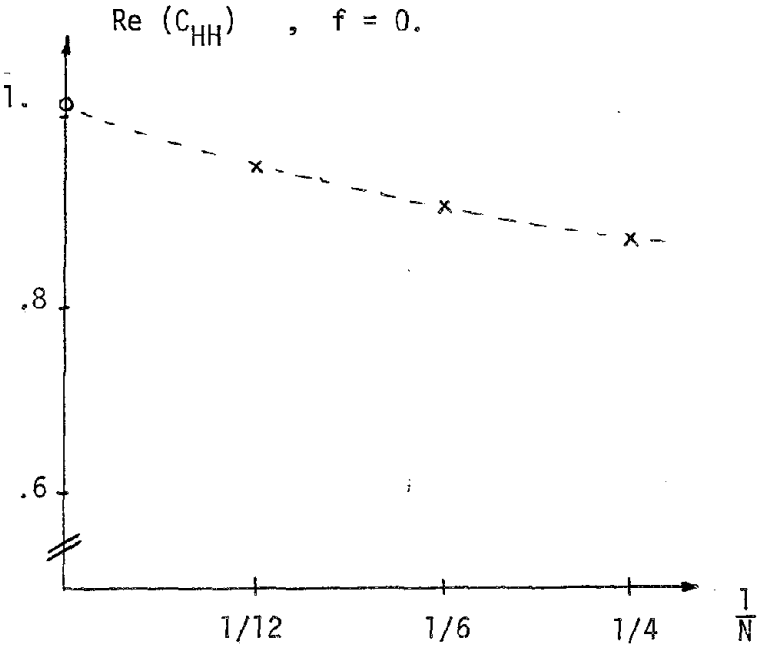
Re (C_{HH}) , f = 0.
1.
.8
.6
1/12
1/6
1/4
$\frac{1}{N}$

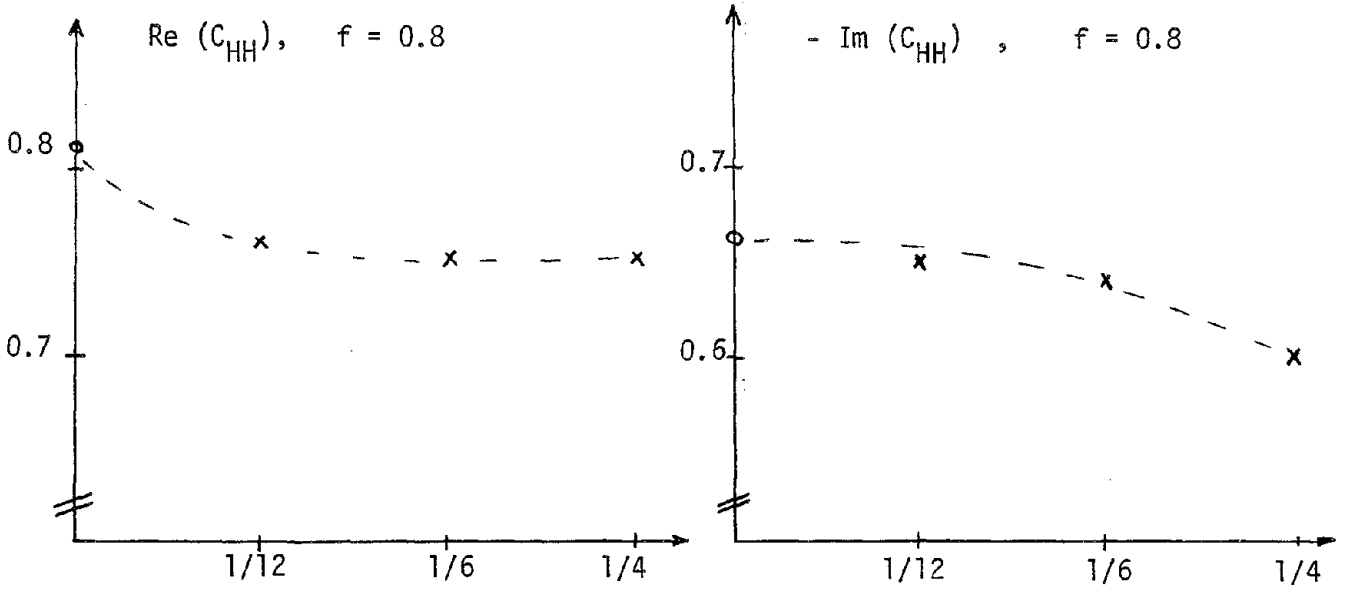
Re (C_{HH}), f = 0.8
0.8
0.7
1/12
1/6
1/4
- Im (C_{HH}) , f = 0.8
0.7
0.6
1/12
1/6
1/4

Fig. 12

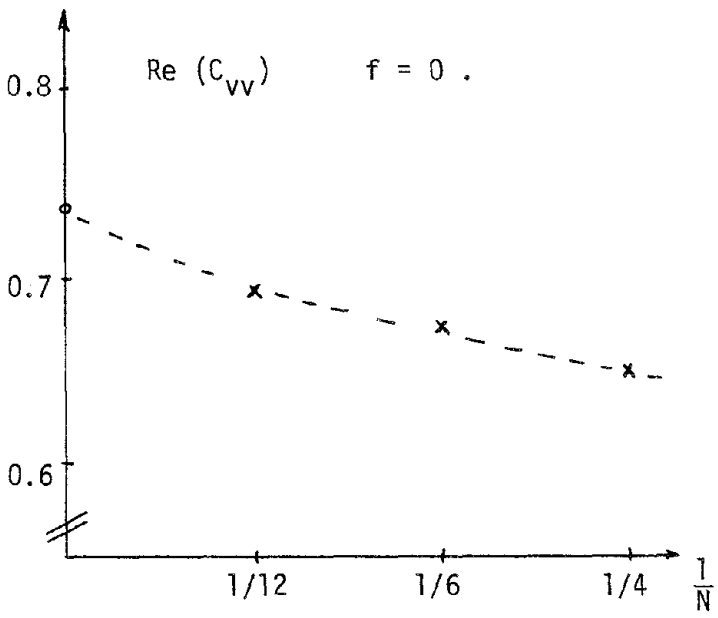
Re (C_{vv}) f = 0 .
0.8
0.7
0.6
1/12
1/6
1/4
$\frac{1}{N}$

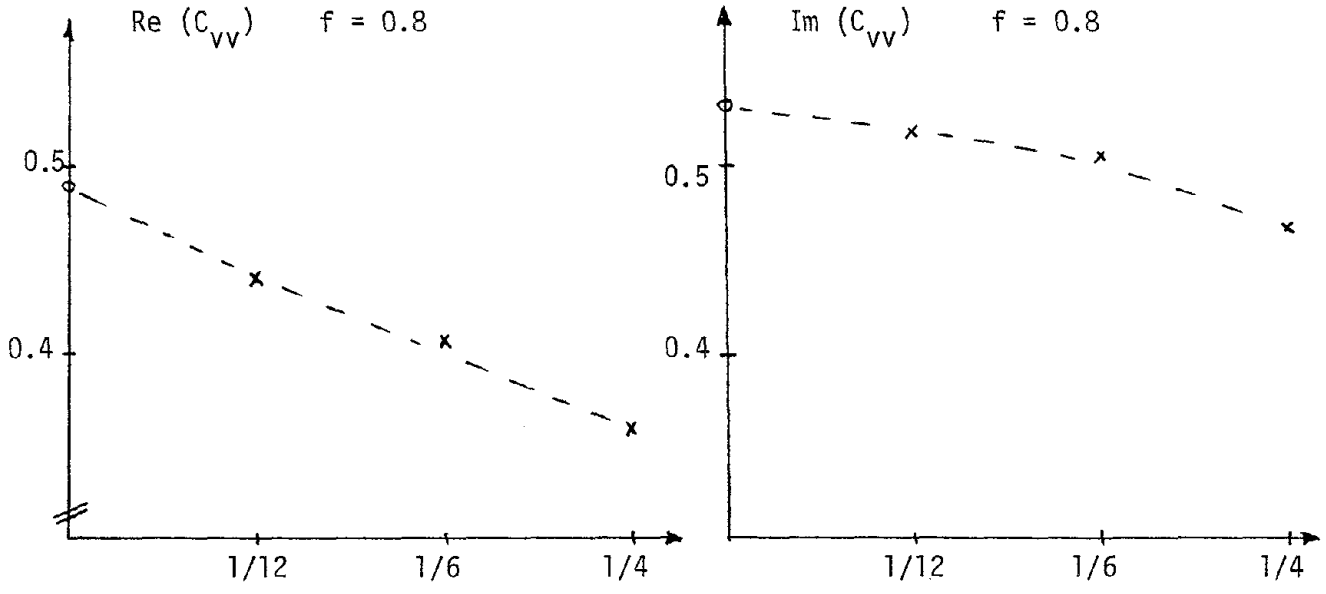
Re (C_{vv}) f = 0.8
0.5
0.4
1/12
1/6
1/4
Im (C_{vv}) f = 0.8
0.5
0.4
1/12
1/6
1/4

Fig. 13

some distance from the load. It can also be observed that the discrete solution begins diverging when the frequency exceeds the limit at which waves with wavelengths shorter than approximately 4h (four times the sublayer thickness) become dominant. In the particular case considered here, this frequency may be estimated as follows.

Considering plane shear waves with frequency f and wavelength λ, we have

$$f\lambda = C_s$$

in which

$$\lambda \geq 4h = 4\,\frac{H}{N}$$

Thus

$$\frac{4H}{N} \leq \frac{C_s}{f}$$

and from here

$$f_o = \frac{fH}{C_s} \leq \frac{N}{4} \quad .$$

For N = 4, this gives a limiting dimensionless frequency $f_o = 1$.

While the execution times of the programs implementing the discrete and "exact" solutions are comparable in the simple case of a homogeneous stratum that was considered in the above examples, the advantage becomes clearly evident in the case of a layered soil, and when the Green functions are required at many different points. The effort associated with evaluating the Green functions with the discrete algorithms is only a function of the number of discrete layers, whether or not they have identical properties; in the "exact" scheme, on the other hand, the effort increases significantly, and difficulties arise in the numerical evaluation of the transforms, because of the greater waviness of the kernels. Thus, the discrete scheme is particularly attractive in the multilayered situation and/or when loads are specified at multiple elevations.

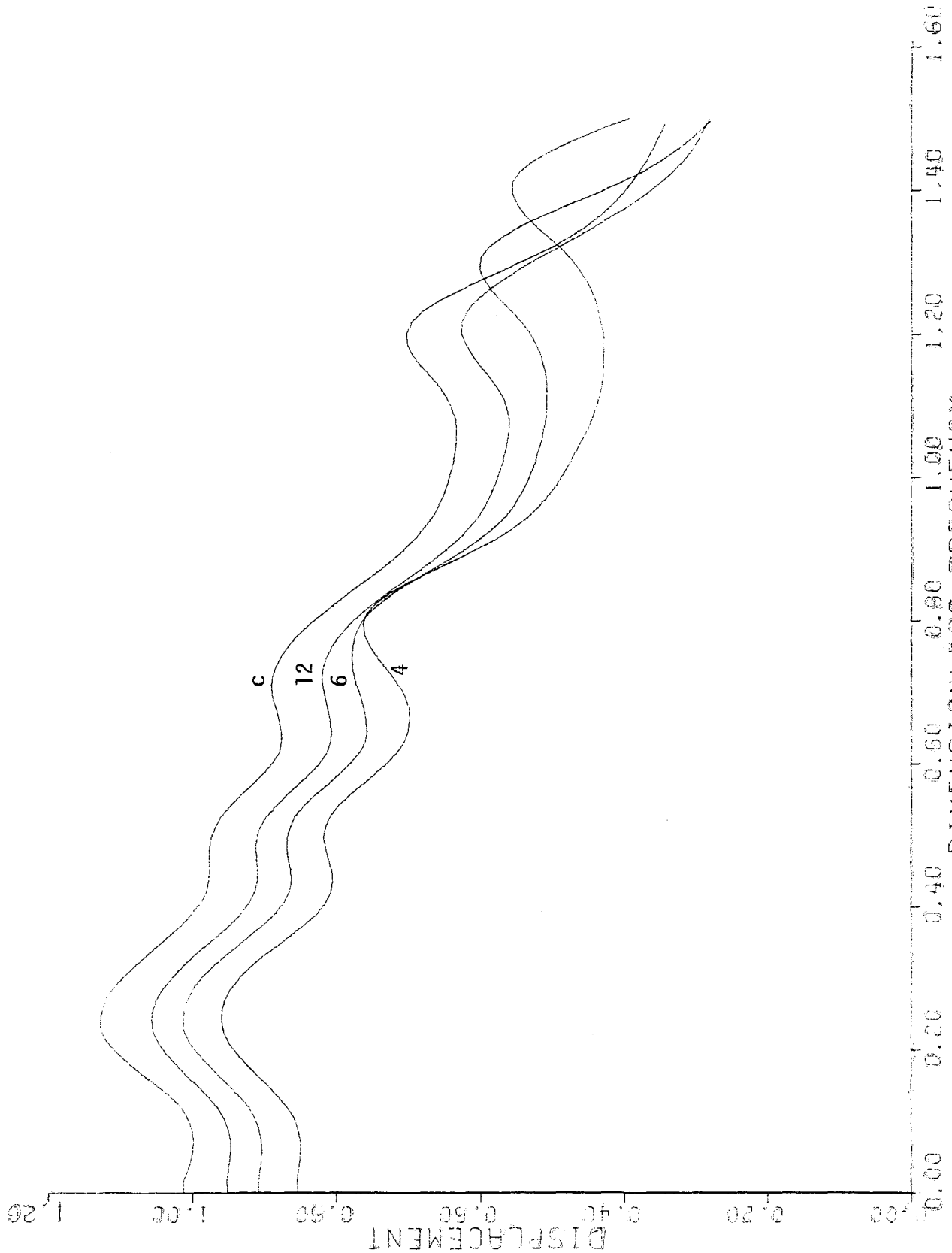

Fig. 14 Real part of horizontal displacement at x = 0, y = 0, z = 0. Horizontal disk load of radius R = 0.25 at the surface.

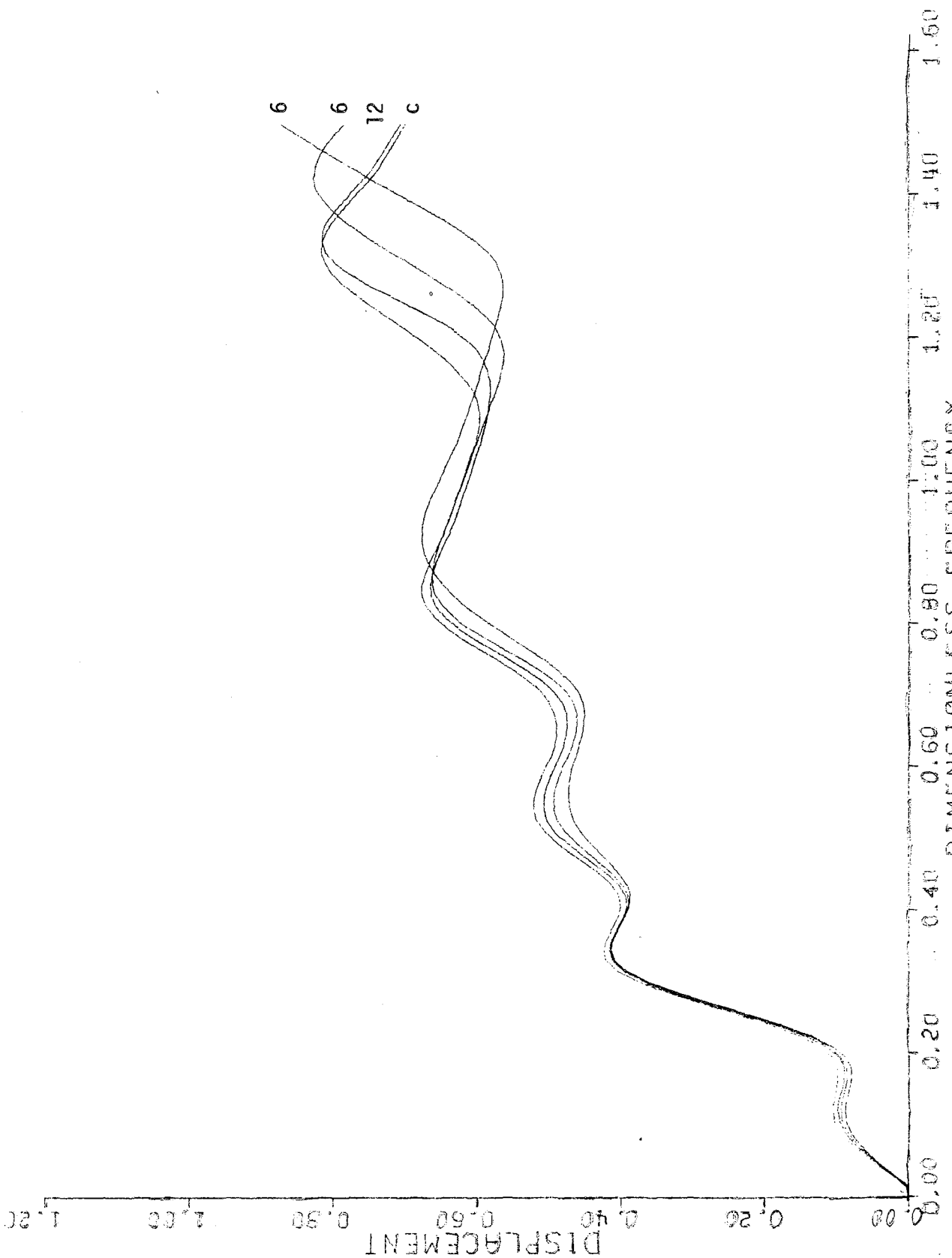

Fig. 15 (-)Imaginary part of horizontal displacement at x = 0, y = 0, z = 0.
Horizontal disk load of radius R = 0.25 at the surface.

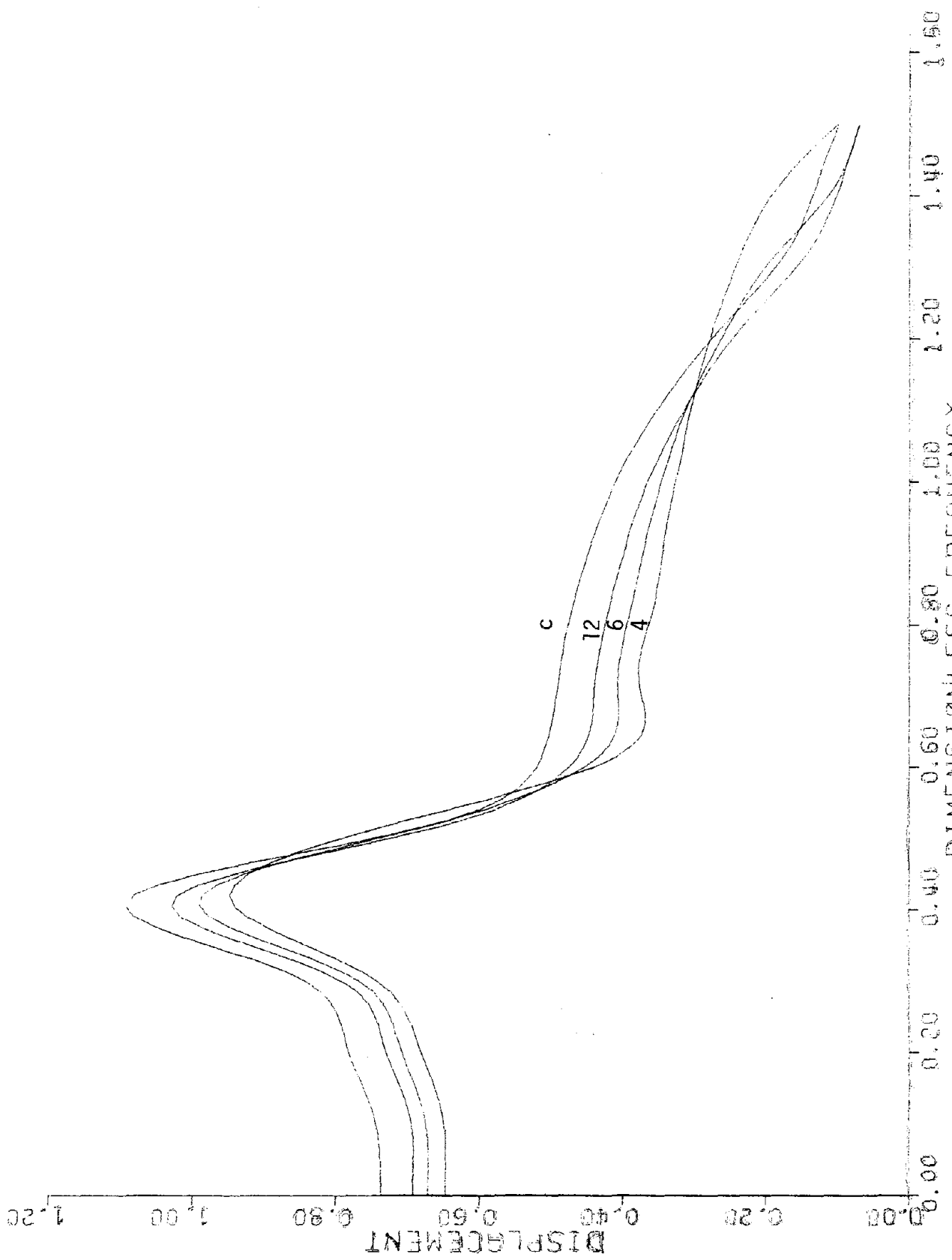

Fig. 16 Real part of vertical displacement at x = 0, y = 0, z = 0, vertical disk load with radius R = 0.25 (at free surface)

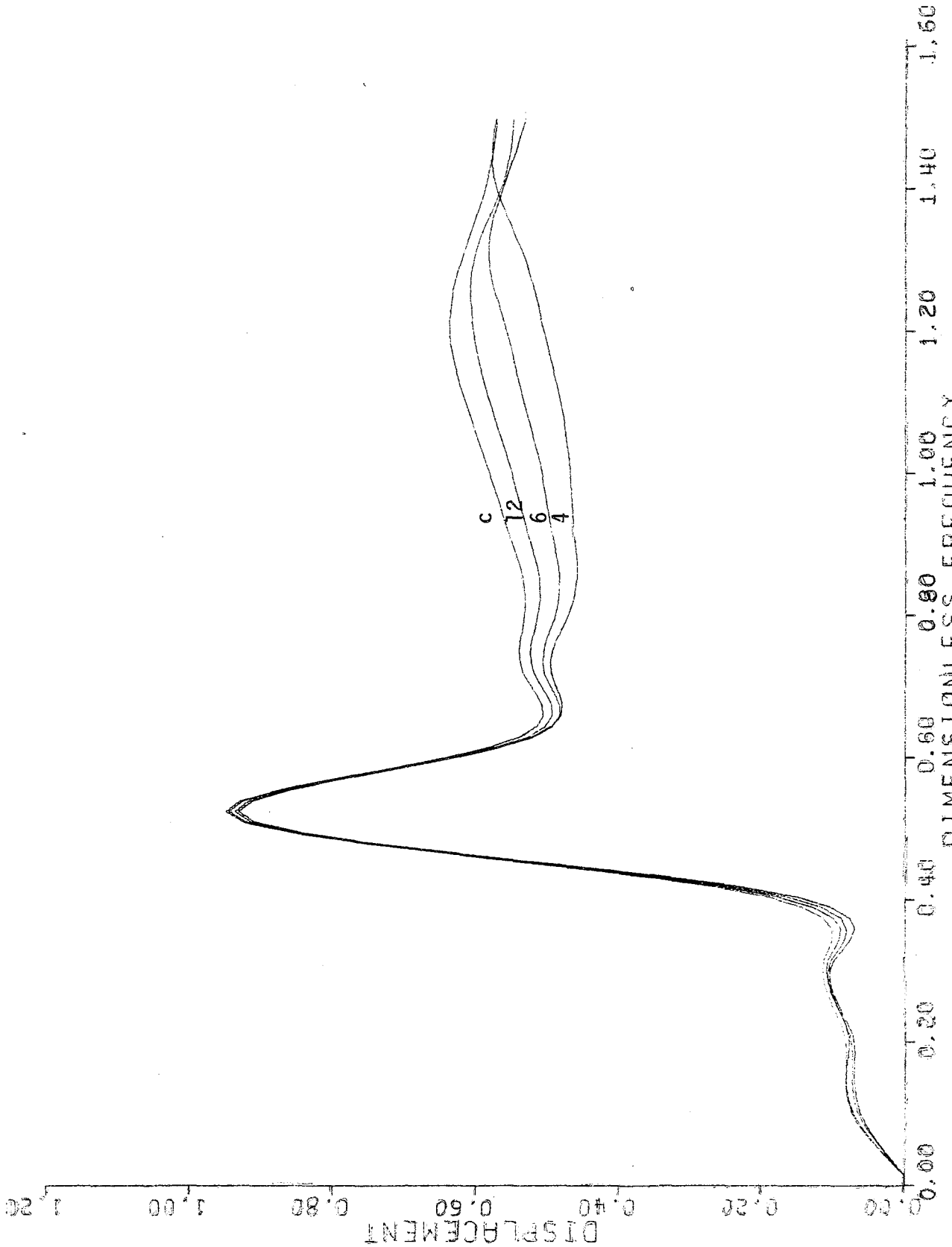

Fig. 17 (-) Imaginary part of vertical displacement at x = 0, y = 0, z = 0, vertical disk load with radius R = 0.25 (at free surface)

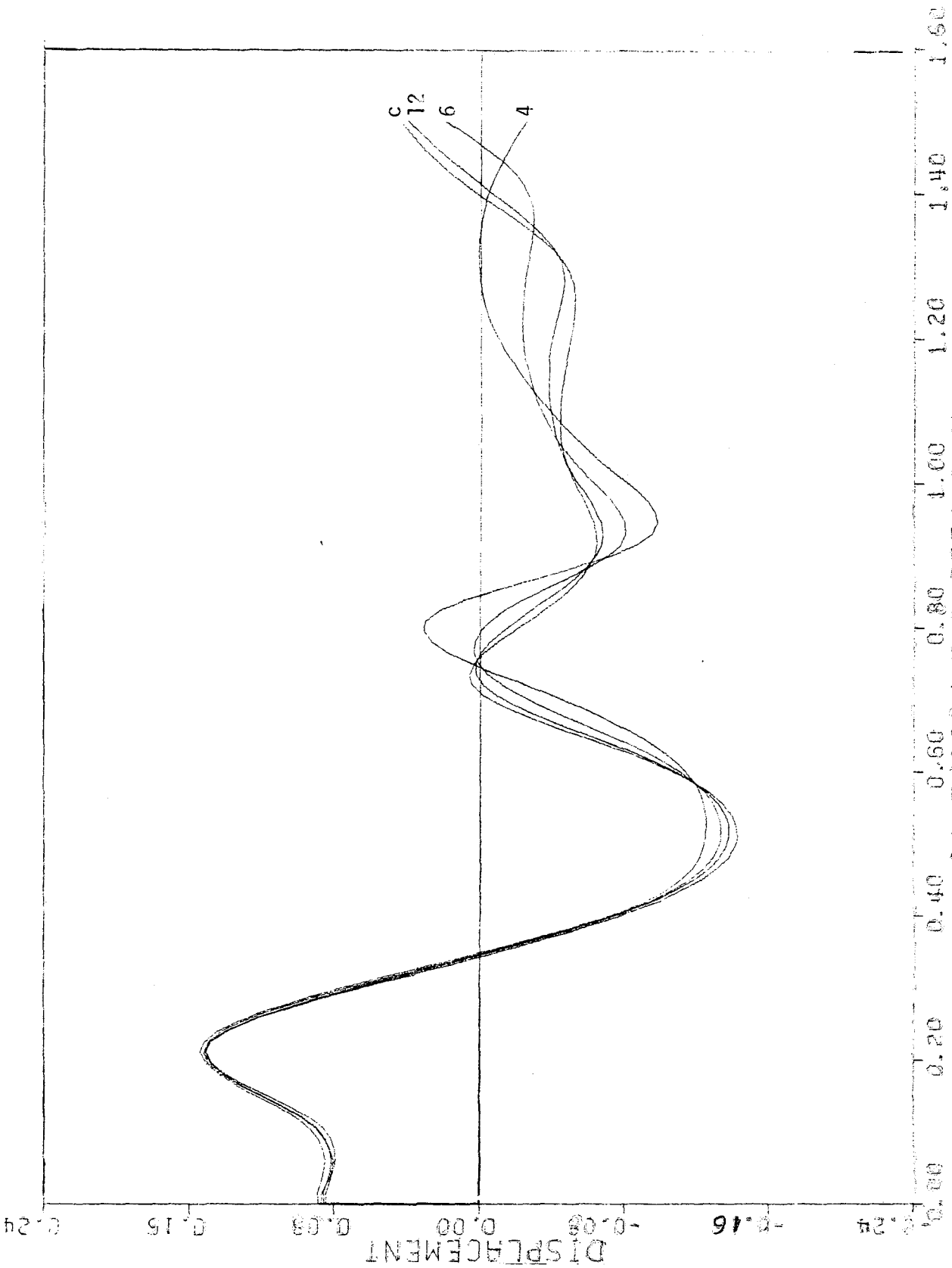

Fig. 18 Real part of the radial displacement at z = 0 (surface), θ = 0, ρ = 1.0 due to a unit horizontal disk load of radius R = 0.25 at the surface.

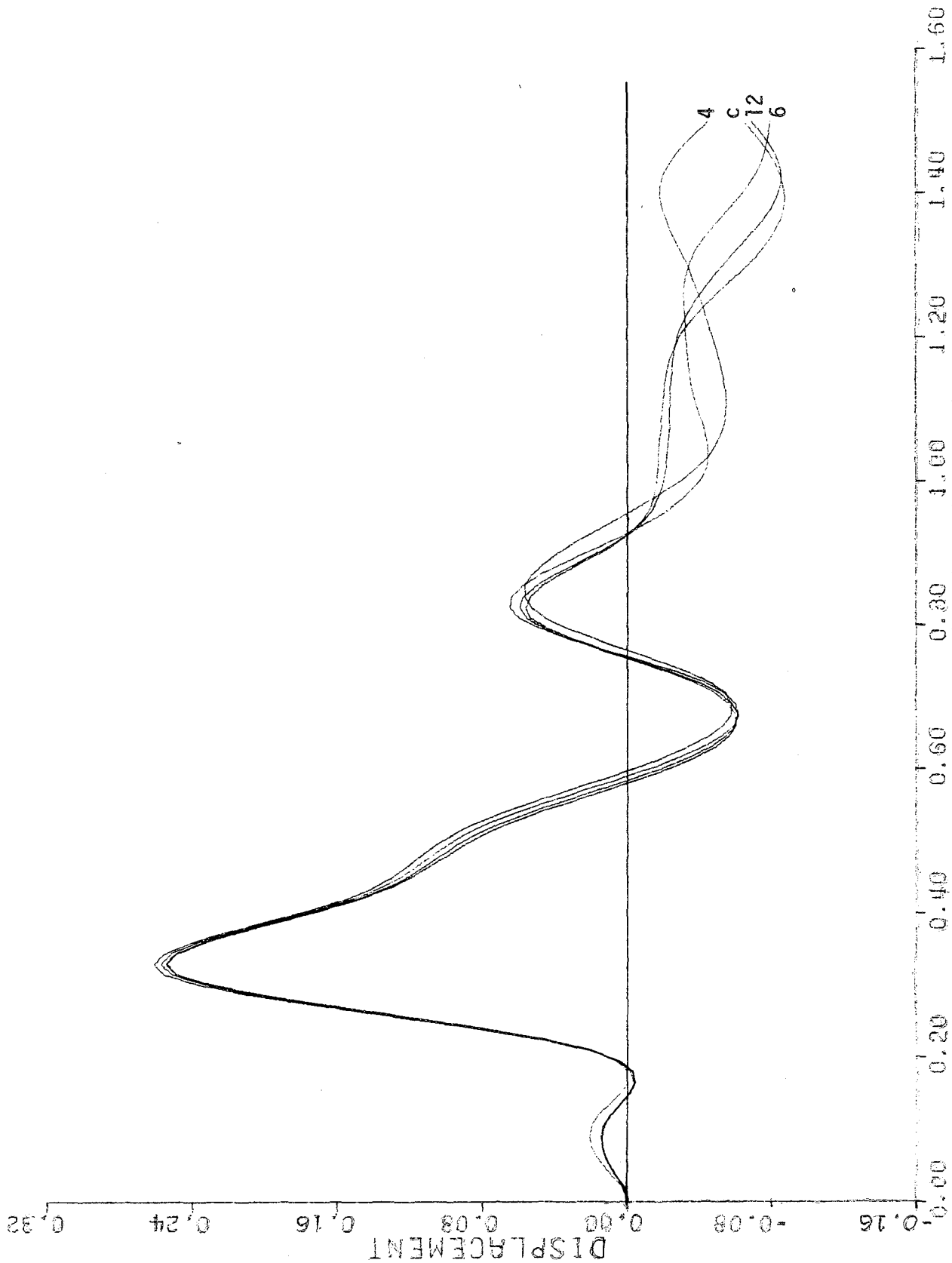

Fig. 19 (-) Imaginary part of radial displacement, at $z = 0$, $\theta = 0$, $\rho = 1$, horizontal disk load of radius $R = 0.25$ (at free surface)

APPENDIX

Current vs. Waas' quadratic eigenvalue problem:

In the original work of Waas (1972), the displacement vector in Cartesian coordinates did not include the factor $i = \sqrt{-1}$ in front of the vertical component, which was in addition taken positive downward. Thus, the quadratic eigenvalue problem corresponding to Eq. (14) had in Waas' work the form

$$(\underset{\sim}{A}\, k^2 + i\, \underset{\sim}{B}\, k + \underset{\sim}{C})\, V = 0 \tag{171}$$

with symmetric matrices $\underset{\sim}{A} \equiv A$, $\underset{\sim}{C} \equiv C$, and an antisymmetric (skew symmetric) matrix $\underset{\sim}{B}$ with the structure

$$\underset{\sim}{B} = \begin{Bmatrix} & -B_{xz} \\ B_{xz}^T & \end{Bmatrix} \tag{172}$$

Also

$$V = \begin{Bmatrix} V_x \\ V_z \end{Bmatrix} = \begin{Bmatrix} \Phi_x \\ i\Phi_z \end{Bmatrix} \tag{173}$$

The modal shapes V were shown by Waas to satisfy the orthogonality relationship

$$K\, \tilde{V}^T A\, V\, K - \tilde{V}^T\, C\, V = 2K^2 \tag{174}$$

which was also used to normalize the eigenvectors. The diagonal matrix K is identical to K_R in the main text. The subscript will be dropped for notation simplicity. The adjoined vector $\tilde{V}$ above is defined as

$$\tilde{V} = \begin{Bmatrix} V_x \\ -V_z \end{Bmatrix} \tag{175}$$

Substituting (173), (175) into (174), we obtain

$$(K\,V_x^T - K\,V_z^T)\begin{bmatrix} A_x & \\ & A_z \end{bmatrix}\begin{Bmatrix} V_x K \\ V_z K \end{Bmatrix} - (V_x^T - V_z^T)\begin{bmatrix} C_x & \\ & C_z \end{bmatrix}\begin{Bmatrix} V_x \\ V_z \end{Bmatrix} = 2K^2 \tag{176}$$

that is,

$$K\,V_x^T A_x\,V_x\,K + V_z^T C_z\,V_z - (K\,V_z^T A_z\,V_z\,K + V_x^T C_x\,V_x) = 2K^2 \tag{177}$$

or using (173),

$$K\,\Phi_x^T A_x\,\Phi_x\,K - \Phi_z^T C_z\,\Phi_z + (K\,\Phi_z^T A_z\,\Phi_z\,K - \Phi_x^T C_x\,\Phi_x) = 2K^2 \tag{178}$$

which is Waas' orthogonality condition in the current notation. On the other hand, the orthogonality condition expressed by Eq. (22) (considering the in-plane problem only, since the antiplane is trivial) is

$$\begin{aligned} Y^T \bar{A}\,Z &= K \\ Y^T \bar{C}\,Z &= -K^3 \end{aligned} \tag{179}$$

or in full

$$(K\,\Phi_x^T \quad \Phi_z^T)\begin{Bmatrix} A_x & \\ B_{xz}^T & A_z \end{Bmatrix}\begin{Bmatrix} \Phi_x & \\ & \Phi_z K \end{Bmatrix} = K \tag{180a}$$

$$(K\Phi_x^T \quad \Phi_z^T)\begin{Bmatrix} C_x & B_{xz} \\ & C_z \end{Bmatrix}\begin{Bmatrix} \Phi_x & \\ & \Phi_z K \end{Bmatrix} = -K^3 \tag{180b}$$

That is,

$$K\,\Phi_x^T A_x\,\Phi_x + \Phi_z^T B_{xz}^T\,\Phi_x + \Phi_z^T A_z\,\Phi_z\,K = K \tag{181a}$$

$$K\,\Phi_x\,C_x\,\Phi_x + K\,\Phi_x^T B_{xz}\,\Phi_z K + \Phi_z^T C_z\,\Phi_z K = -K^3 \tag{181b}$$

Multiplying the first equation by K from the right, followed by a transposition, and the second by K^{-1} from the right, we obtain

$$K\,\Phi_z^T\,A_x\,\Phi_x\,K + K\,\Phi_x^T\,B_{xz}\,\Phi_z + K^2\,\Phi_z^T\,A_z\,\Phi_z = K^2 \tag{182a}$$

$$K\,\Phi_x^T\,C_x\,\Phi_x\,K^{-1} + K\,\Phi_x^T\,B_{xz}\,\Phi_z + \Phi_z^T\,C_z\,\Phi_z = -K^2 \tag{182b}$$

Alternatively, if (181a) is multiplied by K from the left and transposed, and (181b) is multiplied by K^{-1} from the left, we obtain

$$\Phi_x^T\,A_x\,\Phi_x\,K^2 + \Phi_x^T\,B_{xz}\,\Phi_z K + K\,\Phi_z^T\,A_z\,\Phi_z\,K = K^2 \tag{183a}$$

$$\Phi_x^T\,C_x\,\Phi_x + \Phi_x^T\,B_{xz}\,\Phi_z\,K + K^{-1}\,\Phi_z^T\,C_z\,\Phi_z\,K = -K^2 \tag{183b}$$

On the other hand, the eigenvalue Eq. (20a) implies

$$A_x\,\Phi_x\,K^2 + C_x\,\Phi_x + B_{xz}\,\Phi_z K = 0 \tag{184a}$$

$$B_{xz}^T\,\Phi_x\,K^2 + A_z\,\Phi_z\,K^3 + C_z\,\Phi_z\,K = 0 \tag{184b}$$

Multiplying (184a) by Φ_x^T from the left and subtracting from (183a), we obtain

$$K\,\Phi_z^T\,A_z\,\Phi_z\,K - \Phi_x^T\,C_x\,\Phi_x = K^2 \tag{185}$$

Alternatively, multiplying (184b) by K^{-1} from the right, by Φ_z^T from the left, transposing and subtracting from (182a)

$$K\,\Phi_x^T\,A_x\,\Phi_x\,K - \Phi_x^T\,C_z\,\Phi_z = K^2 \tag{186}$$

Addition of (185) and (186) yields then Eq. (177); this proves the equivalence of Waas' orthonormality condition with the one employed in this report.

It remains to prove the other useful relationships that have been used throughout this report.

Consider the first orthogonality condition in Eq. (179):

$$Y^T \bar{A} Z = K \tag{187}$$

If the soil has damping, then all wavenumbers are non-zero, and the inverse of K exists. Thus

$$Z^{-1} \bar{A}^{-1} Y^{-T} = K^{-1} \tag{188}$$

and

$$\bar{A}^{-1} = Z K^{-1} Y^{-T} \tag{189}$$

But

$$\bar{A} = \begin{Bmatrix} A_x & \\ B_{xz}^T & A_z \end{Bmatrix} \tag{190}$$

and

$$\bar{A}^{-1} = \begin{Bmatrix} A_x^{-1} & \\ -A_z^{-1} B_{xz}^T A_x^{-1} & A_z^{-1} \end{Bmatrix} \tag{191}$$

Also, the right-hand side of Eq. (189) is in expanded form:

$$\begin{Bmatrix} \Phi_x \\ \Phi_z K \end{Bmatrix} K^{-1} \begin{Bmatrix} K \Phi_x^T & \Phi_z^T \end{Bmatrix} = \begin{Bmatrix} \Phi_x \Phi_x^T & \Phi_x K^{-1} \Phi_z^T \\ \Phi_z K \Phi_x^T & \Phi_z \Phi_z^T \end{Bmatrix} \tag{192}$$

Comparison of (191) and (192) yields then

$$\left.\begin{aligned} A_x^{-1} &= \Phi_x \Phi_x^T \\ A_z^{-1} &= \Phi_z \Phi_z^T \\ A_z^{-1} B_{xz}^T A_x^{-1} &= -\Phi_z K \Phi_x^T \\ 0 &= \Phi_x K^{-1} \Phi_z^T \end{aligned}\right\} \tag{193}$$

An analogous operation with the second orthogonality condition

$$Y^T \bar{C} Z = -K^3 \tag{194}$$

results in the following expression:

$$\begin{Bmatrix} C_x^{-1} & C_x^{-1} B_{xz} C_z^{-1} \\ & C_z^{-1} \end{Bmatrix} = - \begin{Bmatrix} \Phi_x K^{-2} \Phi_x^T & \Phi_x K^{-3} \Phi_z^T \\ \Phi_z K^{-1} \Phi_x^T & \Phi_z K^{-2} \Phi_z^T \end{Bmatrix}$$

This implies

$$\left.\begin{aligned} C_x^{-1} &= - \Phi_x K^{-2} \Phi_x^T \\ C_z^{-1} &= - \Phi_z K^{-2} \Phi_z^T \\ C_x^{-1} B_{xz} C_z^{-1} &= \Phi_x K^{-3} \Phi_z^T \\ 0 &= \Phi_z K^{-1} \Phi_x^T \end{aligned}\right\} \tag{195}$$

Equations (193) and (195) give then the relationships:

$$\left.\begin{aligned} A_x \Phi_x \Phi_x^T &= I \\ A_z \Phi_z \Phi_z^T &= I \\ A_x \Phi_x K \Phi_z^T A_z &= - B_{xz} \\ C_x \Phi_x K^{-2} \Phi_x^T &= - I \\ C_z \Phi_z K^{-2} \Phi_z^T &= - I \\ C_x \Phi_x K^{-3} \Phi_z^T C_z &= B_{xz} \\ \Phi_x K^{-1} \Phi_z^T &= 0 \end{aligned}\right\} \tag{196}$$

REFERENCES

1. Apsel, R.J. (1979): "Dynamic Green's Functions for Layered Media and Applications to Boundary-Value Problems," Doctor's Thesis, University of California at San Diego.

2. Boussinesq, J. (1878→1885): Citation No. 67 in Love's treatise on the mathematical theory of elasticity, 4th edition. Dover Press, page 16.

3. Cerruti, V. (1882): Citation No. 68 in Love's treatise on the mathematical theory of elasticity, 4th edition, Dover Press, page 16.

4. Drake, L.A. (1972): "Love and Rayleigh Waves in Non-horizontally Layered Media," BSSA, 62, No. 5, pp. 1241-1258, Oct. 1972.

5. Harkreider, D. (1964): "Surface Waves in Multilayer Elastic Media. Rayleigh and Love Waves from a Body Force," BSSA, 54, No. 2, pp. 627-679, April 1964.

6. Haskell, N.A. (1953): "The Dispersion of Surface Waves on Multilayered Media," BSSA, 43, No. 1, pp. 17-34, Feb. 1953.

7. Kausel, E. (1974): "Forced Vibrations of Circular Foundations on Layered Media," Research Report R74-11, Soils Publication No. 336, Dept. of Civil Engineering, M.I.T., Cambridge, Massachusetts.

8. Kausel, E., and Roesset, J.M. (1981): "Stiffness Matrices for Layered Soils," BSSA, 71, No. 6, Dec. 1981.

9. Kelvin (Lord) (1848): "Displacements due to a Point Load in an Indefinitely Extended Solid," Citation No. 66 in Love's treatise on the mathematical theory of elasticity, 4th edition, Dover Press, page 16.

10. Lamb, H. (1904): "On the Propagation of Tremors over the Surface of an Elastic Solid," Phil. Trans. Royal Soc. of London, Series A, Vol.203.

11. Lysmer, J., and Waas, G. (1972): "Shear Waves in Plane Infinite Structures" Journal of the Engineering Mechanics Division, ASCE, Vol. 18, No. EM1, pp. 85-105, Feb. 1972.

12. Mindlin, R.D. (1936): "Force at a point in the interior of a semi-infinite solid," J. Appl. Phys., Vol. 7, No. 5, pp. 195-202.

13. Schlue, J.W. (1979): "Finite Element Matrices for Seismic Surface Waves in Threedimensional Structures," BSSA, 69, No. 5, pp. 1425-1437, Oct. 1979.

14. Tajimi, H. (1980): "A Contribution to Theoretical Prediction of Dynamic Stiffness of Surface Foundations," Proc. of 7th World Conference on Earthquake Engineering, Istanbul, Turkey, Vol. 5, pp. 105-112.

15. Tassoulas, J.L. (1981): "Elements for the Numerical Analysis of Wave Motion in Layered Media," M.I.T. Research Report R81-2, Order No. 689, Dept. of Civil Engineering, M.I.T., Cambridge, Mass., Feb. 1981.

16. Thomson, W.T. (1950): "Transmission of Elastic Waves through a Stratified Soil Medium," J. Appl. Phys., 21, pp. 89-93, Feb. 1950.

17. Waas, G. (1972): "Linear Two-Dimensional Analysis of Soil Dynamics Problems in Semi-infinite Layer Media," PHD Thesis, Univ. of California, Berkeley, CA.

18. Waas, G. (1980): "Dynamisch Belastete Fundamente auf Geschichtetem Baugrund," VDI Berichte, Nr. 381, pp. 185-189, 1980.